PAPER • OPEN ACCESS

Optimal Gaussian metrology for generic multimode interferometric circuit

New Journal of Physics
The open access journal at the forefront of physics

Deutsche Physikalische Gesellschaft DPG
IOP Institute of Physics

Published in partnership with: Deutsche Physikalische Gesellschaft and the Institute of Physics

OPEN ACCESS

RECEIVED
15 November 2018

REVISED
25 January 2019

ACCEPTED FOR PUBLICATION
11 February 2019

PUBLISHED
19 March 2019

PAPER

Optimal Gaussian metrology for generic multimode interferometric circuit

Teruo Matsubara[1], **Paolo Facchi**[2,3], **Vittorio Giovannetti**[4] and **Kazuya Yuasa**[1,5]

[1] Department of Physics, Waseda University, Tokyo 169-8555, Japan
[2] Dipartimento di Fisica and MECENAS, Università di Bari, I-70126 Bari, Italy
[3] INFN, Sezione di Bari, I-70126 Bari, Italy
[4] NEST, Scuola Normale Superiore and Istituto Nanoscienze-CNR, I-56127 Pisa, Italy
[5] Author to whom any correspondence should be addressed.

E-mail: yuasa@waseda.jp

Keywords: quantum metrology, quantum estimation, quantum Fisher information, Gaussian states, squeezed states, optical circuits

Abstract

Bounds on the ultimate precision attainable in the estimation of a parameter in Gaussian quantum metrology are obtained when the average number of bosonic probes is fixed. We identify the optimal input probe state among generic (mixed in general) Gaussian states with a fixed average number of probe photons for the estimation of a parameter contained in a generic multimode interferometric optical circuit, namely, a passive linear circuit preserving the total number of photons. The optimal Gaussian input state is essentially a single-mode squeezed vacuum, and the ultimate precision is achieved by a homodyne measurement on the single mode. We also reveal the best strategy for the estimation when we are given L identical target circuits and are allowed to apply passive linear controls in between with an arbitrary number of ancilla modes introduced.

1. Introduction

Quantum-mechanical features and quantum effects can drastically improve the accuracy of measurements [1–6]. This is known as *quantum metrology*, and is one of the promising future quantum technologies. In particular, quantum optical measurement schemes using photonic probes have recently been under intense study [1, 3–6], pursuing strategies that allow to beat the standard quantum limit on the measurement accuracy, both theoretically [7–64] and experimentally [65–81].

In a variety of quantum optical metrology settings, the probe sensitivity to the target parameter can be improved by squeezing the state of the input light [7, 8]. Entanglement is also an important keyword in the studies of quantum metrology [4–6]. In these ways, the state of the input probe photons is important for high precision metrology.

There is an interesting class of states of light: *Gaussian states*. From a practical point of view, a variety of Gaussian states are relatively easy to generate in laboratories, and various quantum information tasks have been implemented experimentally using photons in Gaussian states [82–84]. Also from a theoretical point of view, they provide an interesting category of quantum information protocols [82–84]. For these reasons, quantum optical metrology with Gaussian input probe states and/or Gaussian channels has been eagerly investigated [14, 16, 17, 19, 21, 25, 28, 29, 32, 34, 36, 43, 45–47, 49, 51, 55, 59–61, 64].

For instance, the estimation of a single-mode phase shift is studied with pure [14] and mixed [19] Gaussian probes, and some other single-mode Gaussian channels such as squeezing and amplitude-damping are analyzed with general mixed Gaussian probes [34]. The estimation of a single-mode phase shift with general mixed Gaussian probes is discussed in the presence of general Gaussian dissipation [60]. A few specific two-mode Gaussian channels like two-mode squeezing and mode mixing are studied with some particular types of two-mode Gaussian probes [59]. The ultimate precision bound is clarified for generic two-mode passive linear circuits, which preserve the number of photons passing through them (they are Gaussian channels) [47]. A formula for the quantum Fisher information (QFI) valid for any multimode pure Gaussian states is derived and investigated under the condition of intense probe

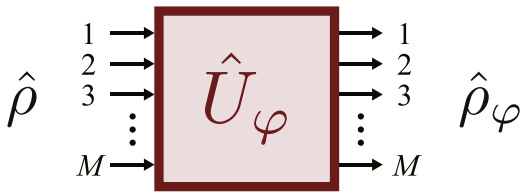

Figure 1. The generic passive linear optical circuit $\hat{U}_\varphi$ with M input ports and M output ports. Our problem is to estimate a parameter φ contained in the circuit $\hat{U}_\varphi$, by sending probe photons through it and measuring its output. We will restrict ourselves to Gaussian input states $\hat{\rho}$ with a given average number of probe photons $\langle\hat{N}\rangle = \overline{N}$, among which we identify the best Gaussian states reducing the accuracy limit in the estimation of φ as much as possible.

light (with large displacement) [25]. General multimode Gaussian unitary channels (Bogoliubov transformations) are considered with pure probe states not restricted to Gaussian states and the behavior of the QFI for large mean photon numbers is discussed [46]. A formula for the QFI matrix is derived for general multimode Gaussian states and multiparameter Gaussian quantum metrology is discussed [61, 64].

In this paper, we study the estimation of a parameter embedded in a generic M-mode passive linear interferometric circuit, and clarify the ultimate precision bound achievable with Gaussian probes. We identify the optimal input probe state among all Gaussian states (including mixed Gaussian states) with a fixed average number of probe photons. Such a bound is known for $M = 2$ [47], but is not known for $M \geqslant 3$. The proof strategy taken for $M = 2$ is not helpful for $M \geqslant 3$, and it is not a simple generalization of the previous work.

More specifically, we will consider the setting shown in figure 1: a collection of M photonic modes is employed as a probe to recover the value of an unknown parameter φ, which is imprinted on the state of the probe via the action of a passive (i.e. photon number preserving), Gaussian (i.e. mapping Gaussian input into Gaussian output), unitary transformation $\hat{U}_\varphi$. Under the assumption that the allowed input density matrices $\hat{\rho}$ of the M modes belong to the set $\mathcal{G}(M, \overline{N})$ of (not necessarily pure) Gaussian states with an average photon number $\overline{N}$, we are interested in the ultimate accuracy in the estimation of φ attainable when having full access to the output state

$$\hat{\rho}_\varphi = \hat{U}_\varphi \hat{\rho} \hat{U}_\varphi^\dagger. \tag{1.1}$$

Our main result consists in showing that, irrespective of the explicit form of $\hat{U}_\varphi$, the minimum value of the uncertainty $\delta\varphi$ on the estimation of φ is bounded from below by the Heisenberg-like scaling

$$\delta\varphi_{\min} \gtrsim 1/\overline{N}. \tag{1.2}$$

To this end, we shall focus on the QFI $F(\varphi|\hat{\rho})$ of the problem, which, via the quantum Cramér–Rao inequality [1, 4, 85–90], sets a universal bound on $\delta\varphi_{\min}$ that is independent of the adopted measurement procedure,

$$\delta\varphi_{\min} \geqslant \frac{1}{\sqrt{F(\varphi|\hat{\rho})}}. \tag{1.3}$$

We hence prove (1.2) by showing that the maximum value of $F(\varphi|\hat{\rho})$ attainable on the set $\mathcal{G}(M, \overline{N})$ is bounded by a quantity which scales quadratically in $\overline{N}$, namely,

$$F(\varphi|\hat{\rho}) \leqslant 8\|g_\varphi\|^2 \overline{N}(\overline{N}+1), \quad \forall\, \hat{\rho} \in \mathcal{G}(M, \overline{N}). \tag{1.4}$$

Here, $\|g_\varphi\|$ is the spectral norm of the Hermitian matrix

$$g_\varphi = \mathrm{i} U_\varphi^\dagger \frac{\mathrm{d}U_\varphi}{\mathrm{d}\varphi}, \tag{1.5}$$

with U_φ being the unitary matrix describing the circuit, defined in (2.2), and is independent of the input state $\hat{\rho}$.

Moreover, we show that the bound (1.4) is sharp and can be saturated. In fact, we identify the optimal states within $\mathcal{G}(M, \overline{N})$ that saturate the inequality (1.4): they are pure states $\rho_{\mathrm{opt}} = |\psi_{\mathrm{opt}}\rangle\langle\psi_{\mathrm{opt}}|$ given in (3.31). We note that, apart from some special cases, such optimal vectors $|\psi_{\mathrm{opt}}\rangle$ generally depend on the variable φ, whose unknown value we wish to determine. Therefore, the possibility of using this optimal input state for achieving the bound is not straightforward, and would require in practice the use of iterative procedures with a sequence of input states that approximate the optimal state. Anyway, the optimal state $|\psi_{\mathrm{opt}}\rangle$ enables us to reach the upper bound (1.4).

The paper is organized as follows. The model and the estimation problem are set up in section 2. In section 3, the maximal precision achievable by a Gaussian probe is found, first for pure Gaussian states and then for mixed Gaussian states. Moreover, we explicitly find the optimal states that achieve the maximal precision. Two different measurement schemes are presented in section 4. We look at a few simple examples in section 5.

Furthermore, in section 6, we exhibit the optimal sequential strategy for the estimation when several target circuits, together with ancilla modes, are allowed to be used. A summary of the present work is given in section 7. We add four appendices, containing some technical tools and proofs. In appendix A we collect some results on Gaussian states and operations, in appendix B we show the derivation of a formula for the QFI, in appendix C we prove some inequalities on Hermitian matrices used in the solution of the optimization problems, and appendix D contains the proof of the optimality of the measurement scheme presented in section 4.

2. The model

Let us consider a set of M bosonic modes described by the operators $\hat{a}_m$ and $\hat{a}_m^\dagger$ satisfying the canonical commutation relations

$$[\hat{a}_m, \hat{a}_n] = 0, \qquad [\hat{a}_m, \hat{a}_n^\dagger] = \delta_{mn} \qquad (m, n = 1, \ldots, M). \tag{2.1}$$

The passive Gaussian unitary $\hat{U}_\varphi$ of figure 1 is defined by the mapping [82, 84]

$$\hat{U}_\varphi^\dagger \hat{a}_m \hat{U}_\varphi = \sum_{n=1}^{M} (U_\varphi)_{mn} \hat{a}_n \qquad (m = 1, \ldots, M), \tag{2.2}$$

or simply written as $\hat{U}_\varphi^\dagger \hat{\boldsymbol{a}} \hat{U}_\varphi = U_\varphi \hat{\boldsymbol{a}}$ with $\hat{\boldsymbol{a}} = (\, \hat{a}_1 \ \cdots \ \hat{a}_M \,)^T$, where U_φ is an $M \times M$ unitary matrix, whose functional dependence upon φ is assumed to be smooth. We remind that this kind of transformation preserves the total number of photons of the system, i.e.

$$\hat{U}_\varphi^\dagger \hat{N} \hat{U}_\varphi = \hat{N}, \qquad \hat{N} = \sum_{m=1}^{M} \hat{a}_m^\dagger \hat{a}_m, \tag{2.3}$$

and can be constructed by using beam splitters and phase shifters.

Our problem is to estimate the actual value of the parameter φ embedded in $\hat{U}_\varphi$ by probing the output state $\hat{\rho}_\varphi$ in (1.1). Consider hence a generic positive operator-valued measure (POVM) $\mathcal{P} = \{\hat{\Pi}_s\}_s$ [91, 92] producing measurement outcomes s with probabilities

$$p(s|\varphi) = \mathrm{Tr}(\hat{\Pi}_s \hat{\rho}_\varphi). \tag{2.4}$$

The Cramér–Rao inequality [1, 4, 85–90] establishes that any attempt at estimating φ from the values of s is characterized by an uncertainty

$$\delta\varphi \geqslant \frac{1}{\sqrt{F(\varphi|\mathcal{P}, \hat{\rho})}}, \tag{2.5}$$

with

$$F(\varphi|\mathcal{P}, \hat{\rho}) = \sum_s p(s|\varphi) \left(\frac{\partial}{\partial\varphi} \ln p(s|\varphi) \right)^2 \tag{2.6}$$

being the Fisher information (FI) of the process. A stronger, universal bound on the attainable estimation error can now be obtained by optimizing the right-hand side of (2.5) with respect to all possible POVMs $\mathcal{P}$. This yields the quantum Cramér–Rao inequality (1.3), with

$$F(\varphi|\hat{\rho}) = \max_{\mathcal{P}} F(\varphi|\mathcal{P}, \hat{\rho}) \tag{2.7}$$

being the QFI of the problem, which by construction depends only upon the input state $\hat{\rho}$ and the circuit $\hat{U}_\varphi$ [1, 4, 85–90]. The maximization in (2.7) can be analytically solved, yielding the following compact expression

$$F(\varphi|\hat{\rho}) = \mathrm{Tr}(\hat{\rho}_\varphi \hat{L}_\varphi^2), \tag{2.8}$$

with $\hat{L}_\varphi$ being a Hermitian operator called symmetric logarithmic derivative (SLD), satisfying

$$\frac{\mathrm{d}\hat{\rho}_\varphi}{\mathrm{d}\varphi} = \frac{1}{2}(\hat{L}_\varphi \hat{\rho}_\varphi + \hat{\rho}_\varphi \hat{L}_\varphi). \tag{2.9}$$

The goal of the present work is to optimize the value of the QFI $F(\varphi|\hat{\rho})$ in (2.8) with respect to a special class of allowed input states $\hat{\rho}$. In particular, we shall restrict the analysis to the set $\mathcal{G}(M, \overline{N})$ of M-mode Gaussian states with a fixed average photon number $\overline{N}$, i.e.

$$\mathrm{Tr}(\hat{N}\hat{\rho}) = \overline{N}. \tag{2.10}$$

This last condition is motivated by the fact that it is not realistic to consider probing signals with unbounded input energy. It turns out that for generic (non-Gaussian) input states the constraint (2.10) is not strong enough to keep the QFI $F(\varphi|\hat{\rho})$ finite (see for instance [47], where, for the case with $M = 2$ input modes, obtaining finite

optimal values for $F(\varphi|\hat{\rho})$ requires to impose an extra condition on the variance of $\hat{N}$ on $\hat{\rho}$; see also [27]), yet for Gaussian inputs this suffices and the QFI $F(\varphi|\hat{\rho})$ is finite under the constraint (2.10).

3. Optimization of QFI

As recapitulated in appendix A, an input state $\hat{\rho}$ belonging to the Gaussian set $\mathcal{G}(M, \overline{N})$ is fully characterized by a ($2M \times 2M$ real, symmetric, and positive-definite) covariance matrix Γ with matrix elements

$$\Gamma_{mn} = \frac{1}{2}\langle\{\hat{z}_m, \hat{z}_n\}\rangle - \langle\hat{z}_m\rangle\langle\hat{z}_n\rangle \qquad (m, n = 1, \ldots, 2M) \tag{3.1}$$

and a ($2M$ real column) displacement vector

$$\boldsymbol{d} = \langle\hat{\boldsymbol{z}}\rangle \tag{3.2}$$

which satisfy the constraint (2.10), i.e.

$$\frac{1}{2}\mathrm{Tr}\left(\Gamma - \frac{1}{2}\right) + \frac{1}{2}\boldsymbol{d}^2 = \overline{N}, \tag{3.3}$$

where $\hat{\boldsymbol{z}} = (\hat{\boldsymbol{x}}\ \ \hat{\boldsymbol{y}})^T$ is the quadrature operator vector with $\hat{x}_m = (\hat{a}_m + \hat{a}_m^\dagger)/\sqrt{2}$ and $\hat{y}_m = (\hat{a}_m - \hat{a}_m^\dagger)/\sqrt{2}\,\mathrm{i}$ ($m = 1, \ldots, M$), and $\langle\cdots\rangle$ denotes the expectation value on $\hat{\rho}$. Furthermore, since $\hat{U}_\varphi$ is a passive Gaussian unitary, the associated output state $\hat{\rho}_\varphi$ obtained as (1.1) also belongs to $\mathcal{G}(M, \overline{N})$, and its covariance matrix Γ_φ and displacement vector $\boldsymbol{d}_\varphi$ depend linearly on Γ and $\boldsymbol{d}$, as

$$\Gamma_\varphi = R_\varphi \Gamma R_\varphi^T, \qquad \boldsymbol{d}_\varphi = R_\varphi \boldsymbol{d}, \tag{3.4}$$

where R_φ is the orthogonal matrix rotating the quadrature operators according to $\hat{U}_\varphi$ (see appendix A). Under this condition, the SLD fulfilling (2.9) can be expressed as [29]

$$\hat{L}_\varphi = (\hat{\boldsymbol{z}} - \boldsymbol{d}_\varphi)^T \Lambda_\varphi (\hat{\boldsymbol{z}} - \boldsymbol{d}_\varphi) + \frac{\partial \boldsymbol{d}_\varphi^T}{\partial\varphi}\Gamma_\varphi^{-1}(\hat{\boldsymbol{z}} - \boldsymbol{d}_\varphi) - \mathrm{Tr}(\Lambda_\varphi\Gamma_\varphi), \tag{3.5}$$

and, accordingly, the QFI reads [29, 93]

$$F(\varphi|\hat{\rho}) = \mathrm{Tr}\left(\Lambda_\varphi \frac{\partial\Gamma_\varphi}{\partial\varphi}\right) + \frac{\partial \boldsymbol{d}_\varphi^T}{\partial\varphi}\Gamma_\varphi^{-1}\frac{\partial \boldsymbol{d}_\varphi}{\partial\varphi}. \tag{3.6}$$

Here, Λ_φ is the solution to

$$\mathrm{i}J\Lambda_\varphi - (2\Gamma_\varphi \mathrm{i}J)^{-1}\mathrm{i}J\Lambda_\varphi(2\Gamma_\varphi \mathrm{i}J)^{-1} = -\frac{\partial(2\Gamma_\varphi \mathrm{i}J)^{-1}}{\partial\varphi}, \tag{3.7}$$

with J being the $2M \times 2M$ matrix

$$J = \begin{pmatrix} 0 & \mathbb{I} \\ -\mathbb{I} & 0 \end{pmatrix}, \tag{3.8}$$

known as the symplectic form.

In the remainder of this section, we shall employ these expressions to derive the inequality (1.4). The analysis will be split into two parts, addressing first the case of the pure elements of $\mathcal{G}(M, \overline{N})$ and then the case of the mixed ones. For those who are familiar with QFI optimization problems, this procedure might sound unnecessary. Indeed, due to the convexity of QFI [4, 94], it is well-known that pure input states perform better than mixed input states for metrological purposes. We cannot, however, apply the same argument in the present case, and it is not obvious at first glance whether the best state is a pure state. Indeed, even though it is true that any mixed Gaussian state can be decomposed as a convex sum of pure Gaussian states, each of the constituent of such decomposition does not necessarily satisfy the constraint (2.10) on the photon number in general. In short, the Gaussian set $\mathcal{G}(M, \overline{N})$ is not a convex set, and therefore we cannot use the convexity argument to optimize the QFI. As a consequence, for the problem we are considering here, we have to address explicitly the case of mixed input states.

3.1. Optimization among pure Gaussian inputs

For a pure Gaussian state $|\psi\rangle \in \mathcal{G}(M, \overline{N})$, the symplectic eigenvalues of its covariance matrix Γ (i.e. the parameters $\{\sigma_1, \ldots, \sigma_M\}$ in the canonical decomposition (A.10) of Γ) are all equal to $\sigma_m = 1/2$ ($m = 1, \ldots, M$). Accordingly, introducing a $2M \times 2M$ symplectic orthogonal matrix R (i.e. an orthogonal matrix R satisfying $R^T J R = J$) and an $M \times M$ diagonal positive matrix r, the covariance matrix Γ can be decomposed as (see the canonical decomposition (A.10) of Γ of a generic (mixed) Gaussian state)

$$\Gamma = \frac{1}{2}RQ^2R^T = \frac{1}{2}R\begin{pmatrix} \mathrm{e}^{r} & 0 \\ 0 & \mathrm{e}^{-r} \end{pmatrix}^2 R^T, \tag{3.9}$$

while the constraint (3.3) on the average number becomes

$$\mathrm{Tr}(\sinh^2 r) + \frac{1}{2}\boldsymbol{d}^2 = \overline{N}, \tag{3.10}$$

with $\boldsymbol{d}$ being the displacement vector of $|\psi\rangle$.

Exactly the same properties hold for the covariance matrix Γ_φ and the displacement $\boldsymbol{d}_\varphi$ of the associated output counterpart (1.1) of $|\psi\rangle$, which of course is also a pure element of the set $\mathcal{G}(M, \overline{N})$. Under this premise, the equation (3.7) for Λ_φ can be solved explicitly, yielding

$$\Lambda_\varphi = -\frac{1}{4}\frac{\partial\Gamma_\varphi^{-1}}{\partial\varphi}. \tag{3.11}$$

The QFI (3.6) is then reduced to [29]

$$F(\varphi|\hat{\rho}) = \frac{1}{4}\mathrm{Tr}\left[\left(\Gamma_\varphi^{-1}\frac{\partial\Gamma_\varphi}{\partial\varphi}\right)^2\right] + \frac{\partial\boldsymbol{d}_\varphi^T}{\partial\varphi}\Gamma_\varphi^{-1}\frac{\partial\boldsymbol{d}_\varphi}{\partial\varphi}, \tag{3.12}$$

with the SLD (3.5) given by

$$\hat{L}_\varphi = -\frac{1}{4}(\hat{\boldsymbol{z}} - \boldsymbol{d}_\varphi)^T\frac{\partial\Gamma_\varphi^{-1}}{\partial\varphi}(\hat{\boldsymbol{z}} - \boldsymbol{d}_\varphi) + \frac{\partial\boldsymbol{d}_\varphi^T}{\partial\varphi}\Gamma_\varphi^{-1}(\hat{\boldsymbol{z}} - \boldsymbol{d}_\varphi) - \frac{1}{4}\mathrm{Tr}\left(\Gamma_\varphi^{-1}\frac{\partial\Gamma_\varphi}{\partial\varphi}\right). \tag{3.13}$$

A further simplification can then be obtained by invoking (3.4), which expresses the functional dependence of Γ_φ and $\boldsymbol{d}_\varphi$ in terms of the symplectic orthogonal matrix R_φ representing the passive Gaussian unitary transformation $\hat{U}_\varphi$. Specifically, we get

$$F(\varphi|\hat{\rho}) = \frac{1}{2}\mathrm{Tr}(G_\varphi\Gamma^{-1}G_\varphi\Gamma - G_\varphi^2) + \boldsymbol{d}^TG_\varphi\Gamma^{-1}G_\varphi\boldsymbol{d}, \tag{3.14}$$

and

$$\hat{L}_\varphi = \frac{\mathrm{i}}{4}(R_\varphi^T\hat{\boldsymbol{z}} - \boldsymbol{d})^T[G_\varphi, \Gamma^{-1}](R_\varphi^T\hat{\boldsymbol{z}} - \boldsymbol{d}) + \mathrm{i}\boldsymbol{d}^TG_\varphi\Gamma^{-1}(R_\varphi^T\hat{\boldsymbol{z}} - \boldsymbol{d}), \tag{3.15}$$

where

$$G_\varphi = \mathrm{i}R_\varphi^T\frac{\mathrm{d}R_\varphi}{\mathrm{d}\varphi} \tag{3.16}$$

is the generator of R_φ.

Our problem is, therefore, to maximize the QFI $F(\varphi|\hat{\rho})$ in (3.14) with respect to Γ and $\boldsymbol{d}$, keeping in mind the parameterization (3.9) and the constraint (3.10). For this purpose, we start bounding the first term $F^{(1)}(\varphi|\hat{\rho})$ in the sum (3.14). By plugging the symplectic decomposition (3.9) of Γ, and using the parameterization (A.12) for R as well as the structure (A.21) of the generator G_φ, we get (see appendix B for the derivation)

$$\begin{aligned} F^{(1)}(\varphi|\hat{\rho}) &= \frac{1}{2}\mathrm{Tr}(G_\varphi\Gamma^{-1}G_\varphi\Gamma - G_\varphi^2) \\ &= \mathrm{Tr}[(U^\dagger g_\varphi U\cosh 2r)^2] + \mathrm{Tr}(U^\dagger g_\varphi U\sinh 2r\ U^Tg_\varphi^*U^*\sinh 2r) - \mathrm{Tr}(g_\varphi^2) \end{aligned} \tag{3.17}$$

where g_φ is the generator of the unitary matrix U_φ as introduced in (1.5) and involved in the structure of G_φ in (A.21), while U is the unitary matrix appearing in the parameterization of R in (A.12). This quantity can be bounded from above as

$$\begin{aligned} F^{(1)}(\varphi|\hat{\rho}) &\leqslant \mathrm{Tr}[(U^\dagger g_\varphi U)^2\cosh^2 2r] + \mathrm{Tr}[(U^\dagger g_\varphi U)^2\sinh^2 2r] - \mathrm{Tr}(g_\varphi^2) \\ &= 2\mathrm{Tr}[(U^\dagger g_\varphi U)^2\sinh^2 2r] \\ &\leqslant 2\|g_\varphi\|^2\mathrm{Tr}\sinh^2 2r, \end{aligned} \tag{3.18}$$

where we have used the inequalities

$$\mathrm{Tr}[(AB)^2] \leqslant \mathrm{Tr}(A^2B^2), \tag{3.19}$$

$$\mathrm{Tr}(A^T B^T A B) \leqslant \mathrm{Tr}(A^2 B^2), \tag{3.20}$$

valid for Hermitian matrices A and B, and

$$\mathrm{Tr}(AB) \leqslant \|A\| \,\mathrm{Tr}\, B, \tag{3.21}$$

valid for Hermitian and positive semi-definite matrices A and B (see appendix C for their proofs). Note that g_φ is Hermitian and hence $(U^\dagger g_\varphi U)^2$ is positive semi-definite, and its norm is given by $\|(U^\dagger g_\varphi U)^2\| = \|g_\varphi\|^2$. The equality in (3.19) holds if and only if $[A, B] = 0$, while the equality in (3.20) is obtained if and only if $AB = (AB)^T$.

The second term $F^{(2)}(\varphi|\hat{\rho})$ in (3.14), on the other hand, can be bounded from above as

$$\begin{aligned} F^{(2)}(\varphi|\hat{\rho}) &= \boldsymbol{d}^T G_\varphi \Gamma^{-1} G_\varphi \boldsymbol{d} \\ &= 2\boldsymbol{d}^T G_\varphi R Q^{-2} R^T G_\varphi \boldsymbol{d} \\ &\leqslant 2\|G_\varphi R Q^{-2} R^T G_\varphi\| \boldsymbol{d}^2 \\ &\leqslant 2\|G_\varphi\|^2 \|Q^{-2}\| \boldsymbol{d}^2 \\ &= 2\|g_\varphi\|^2 \|\mathrm{e}^{2r}\| \boldsymbol{d}^2, \end{aligned} \tag{3.22}$$

where we have assumed, without loss of generality, that $r_m \geqslant 0$ $(m = 1, \ldots, M)$.

Exploiting these results, we can then bound the QFI (3.14) as

$$\begin{aligned} F(\varphi|\,\hat{\rho}) &\leqslant 2\|g_\varphi\|^2 (\mathrm{Tr}\sinh^2 2r + \|\mathrm{e}^{2r}\| \boldsymbol{d}^2) \\ &= 2\|g_\varphi\|^2 (4\,\mathrm{Tr}\sinh^2 r + 4\,\mathrm{Tr}\sinh^4 r + \|\mathrm{e}^{2r}\| \boldsymbol{d}^2) \\ &\leqslant 2\|g_\varphi\|^2 [4\,\mathrm{Tr}\sinh^2 r + 4(\mathrm{Tr}\sinh^2 r)^2 + 2\|\cosh 2r\| \boldsymbol{d}^2] \\ &= 2\|g_\varphi\|^2 [4\,\mathrm{Tr}\sinh^2 r + 4(\mathrm{Tr}\sinh^2 r)^2 + (4\|\sinh^2 r\| + 2) \boldsymbol{d}^2] \\ &\leqslant 2\|g_\varphi\|^2 [4\,\mathrm{Tr}\sinh^2 r + 4(\mathrm{Tr}\sinh^2 r)^2 + (4\,\mathrm{Tr}\sinh^2 r + 2) \boldsymbol{d}^2], \end{aligned} \tag{3.23}$$

where we have used the inequality

$$\mathrm{Tr}(A^2) \leqslant (\mathrm{Tr}\, A)^2\,, \tag{3.24}$$

valid for a positive semi-definite matrix A, which is saturated if and only if only one of the eigenvalues of A is nonvanishing and it is not degenerate (see appendix C for its proof). Imposing hence the constraint (3.10), this finally gives us

$$F(\varphi|\hat{\rho}) \leqslant 8\|g_\varphi\|^2 \left(\overline{N}(\overline{N} + 1) - \frac{1}{4}\boldsymbol{d}^4 \right) \leqslant 8\|g_\varphi\|^2 \overline{N}(\overline{N} + 1), \tag{3.25}$$

which proves the inequality (1.4) for the case of pure input Gaussian states. This result reproduces the bounds previously known for $M = 1$ (single-mode phase shift) [14, 19, 34, 40, 59] and for $M = 2$ (general two-mode passive linear circuits) [47], and generalizes them to $M \geqslant 3$.

3.1.1. Optimal states

The above derivation of the bound not only proves that the inequality (1.4) holds at least for the pure input states of the set $\mathcal{G}(M, \overline{N})$, but also that the bound is saturated by a proper choice of the inputs, i.e. by properly tuning the parameters in Γ and $\boldsymbol{d}$. Let us identify such input states.

(i) In order to saturate the last inequality in (3.25), the necessary and sufficient condition is

$$\boldsymbol{d} = 0. \tag{3.26}$$

(ii) Then, the last inequality in (3.23) is automatically saturated, and the second inequality in (3.23) is saturated if and only if only one (e.g. the first) of the squeezing parameters $\{r_1, \ldots, r_M\}$ of the matrix r is nonvanishing. Let us put the nonvanishing squeezing parameter $r_0\,(>0)$ in the first mode,

$$r = \begin{pmatrix} r_0 & & & \\ & 0 & & \\ & & \ddots & \\ & & & 0 \end{pmatrix}. \tag{3.27}$$

(iii) The equality in (3.22) is trivially satisfied, since $\boldsymbol{d}$ is required to be vanishing in (3.26).

(iv) The last inequality in (3.18) is saturated if and only if the vector $(1 \;\; 0 \;\; \cdots \;\; 0)^T$, corresponding to the first mode, belongs to the eigenspace of $(U^\dagger g_\varphi U)^2$ associated with its largest eigenvalue. The choice

$$U = V_\varphi, \tag{3.28}$$

with V_φ introduced in (A.23) to diagonalize g_φ, suffices to fulfill this condition. Note that the eigenvalues $\{\varepsilon_1, \ldots, \varepsilon_M\}$ of g_φ in (A.23) are ordered in descending order in their magnitudes.

(v) The first inequality in (3.18) is saturated if and only if both conditions

$$\begin{cases} [U^\dagger g_\varphi U, \cosh 2r] = 0, \\ U^\dagger g_\varphi U \sinh 2r = (U^\dagger g_\varphi U \sinh 2r)^T \end{cases} \tag{3.29}$$

are satisfied: recall the conditions for the equalities in (3.19) and (3.20). These conditions are already satisfied with the above tunings of r and U in (3.27) and (3.28).

(vi) Finally, since $\boldsymbol{d} = 0$, all the photons are spent for the squeezing r_0 in the first mode. The constraint on the mean photon number $\overline{N}$ in (3.10) yields

$$r_0 = \ln(\sqrt{\overline{N}} + \sqrt{\overline{N}+1}). \tag{3.30}$$

Putting all these conditions together, it follows that the state achieving the upper bound in (3.25) among the pure Gaussian input states of $\mathcal{G}(M, \overline{N})$ is a *single-mode squeezed vacuum* with zero displacement (3.26) and a squeezing r given by (3.27) and (3.30), and rotated by the unitary (3.28), i.e. the vector

$$|\psi_{\rm opt}\rangle = \hat{V}_\varphi \hat{S}_1(r_0)|0\rangle, \tag{3.31}$$

with $|0\rangle$ the vacuum state and $\hat{S}_1(\xi) = \mathrm{e}^{\frac{1}{2}(\xi \hat{a}_1^{\dagger 2} - \xi^* \hat{a}_1^2)}$ the squeezing operator on the first mode.

A couple of comments are in order. First, recall that $\hat{V}_\varphi$ is the passive linear transformation characterized by $\hat{V}_\varphi^\dagger \hat{\boldsymbol{a}} \hat{V}_\varphi = V_\varphi \hat{\boldsymbol{a}}$ with the $M \times M$ unitary matrix V_φ diagonalizing the generator g_φ of the circuit as in (A.23). It redefines the modes of the system in a way that allows us to describe the optimal state as a configuration with all the photons injected into the first mode only (i.e. the one with the largest (in magnitude) eigenvalue of g_φ). We stress, however, that even after this 'reorganization' the modes other than the first one are not free from the target parameter φ in general, due to the subsequent propagation induced by $\hat{U}_\varphi$, and the problem is not reduced to a single-mode problem. It remains intrinsically a multimode problem, and we cannot simply apply the results known for single-mode estimation problems. Second, as indicated by the notation, the transformation $\hat{V}_\varphi$ may depend upon the target parameter φ for a generic choice of $\hat{U}_\varphi$, and so may do the optimal state $|\psi_{\rm opt}\rangle$. Therefore, if that is the case, it would not be easy to prepare this optimal state $|\psi_{\rm opt}\rangle$ without knowing the value of the parameter φ, which we intend to estimate, and an adaptive strategy updating the estimate of φ would be required in practice.

3.2. Optimization among mixed Gaussian inputs

We have just shown that the inequality (1.4) holds at least for the pure elements of the set $\mathcal{G}(M, \overline{N})$. Here, we are going to generalize this by showing that the same result holds for the mixed elements of the set $\mathcal{G}(M, \overline{N})$.

We first point out that any mixed Gaussian state $\hat{\rho}_{\Gamma,\boldsymbol{d}}$, characterized by a covariance matrix Γ and a displacement $\boldsymbol{d}$, can be expressed as a mixture of pure Gaussian states $\hat{\rho}_{\Gamma_0,\boldsymbol{d}-\boldsymbol{\xi}}$ as

$$\hat{\rho}_{\Gamma,\boldsymbol{d}} = \int \mathrm{d}^{2M}\boldsymbol{\xi}\; P_\Gamma(\boldsymbol{\xi}) \hat{\rho}_{\Gamma_0,\boldsymbol{d}-\boldsymbol{\xi}} \tag{3.32}$$

with a Gaussian probability distribution

$$P_\Gamma(\boldsymbol{\xi}) = \frac{\mathrm{e}^{-\frac{1}{2}\boldsymbol{\xi}^T(\Gamma-\Gamma_0)^{-1}\boldsymbol{\xi}}}{\sqrt{(2\pi)^{2M}\det(\Gamma-\Gamma_0)}}. \tag{3.33}$$

In these expressions, Γ_0 is the pure state covariance matrix obtained by taking the symplectic decomposition (A.10) of the original covariance matrix Γ and replacing all the symplectic eigenvalues $\{\sigma_1, \ldots, \sigma_M\}$ of the latter with $1/2$, i.e.

$$\Gamma_0 = \frac{1}{2} R Q^2 R^T, \tag{3.34}$$

keeping the squeezing matrix Q and the symplectic orthogonal matrix R of Γ unchanged. By construction, it follows that

$$\Gamma - \Gamma_0 \geqslant 0, \tag{3.35}$$

since all the symplectic eigenvalues $\{\sigma_1, \ldots, \sigma_M\}$ of any Γ are greater than or equal to $1/2$. The convex decomposition (3.32) can be verified by looking at the characteristic function $\chi_{\Gamma,\boldsymbol{d}}(\boldsymbol{\eta})$ for the Gaussian state $\hat{\rho}_{\Gamma,\boldsymbol{d}}$

in (A.8): by direct computation, we can check that

$$\int \mathrm{d}^{2M}\boldsymbol{\xi}\; P_{\Gamma}(\boldsymbol{\xi})\chi_{\Gamma_0,\boldsymbol{d}-\boldsymbol{\xi}}(\boldsymbol{\eta}) = \chi_{\Gamma,\boldsymbol{d}}(\boldsymbol{\eta}), \tag{3.36}$$

which is equivalent to (3.32). Note that the pure Gaussian states $\hat{\rho}_{\Gamma_0,\boldsymbol{d}-\boldsymbol{\xi}}$ in the convex sum (3.32) do *not* satisfy the constraint (3.3) on the mean photon number in general, while the original mixed state $\hat{\rho}_{\Gamma,\boldsymbol{d}}$ should do. Yet, by using the convexity of the QFI and the last inequality appearing in (3.23), which holds for pure Gaussian states, and by recalling the expressions for the mean photon number in (3.3) and (3.10), we can write

$$\begin{aligned}
F(\varphi|\hat{\rho}_{\Gamma,\boldsymbol{d}}) &\leqslant \int \mathrm{d}^{2M}\boldsymbol{\xi}\; P_{\Gamma}(\boldsymbol{\xi})F(\varphi|\hat{\rho}_{\Gamma_0,\boldsymbol{d}-\boldsymbol{\xi}}) \\
&\leqslant 8\|g_{\varphi}\|^2 \int \mathrm{d}^{2M}\boldsymbol{\xi}\; P_{\Gamma}(\boldsymbol{\xi})\left\{\frac{1}{2}\left[\mathrm{Tr}\left(\Gamma_0-\frac{1}{2}\right)+(\boldsymbol{d}-\boldsymbol{\xi})^2\right]\right. \\
&\quad \left. +\frac{1}{4}\left[\mathrm{Tr}\left(\Gamma_0-\frac{1}{2}\right)+(\boldsymbol{d}-\boldsymbol{\xi})^2\right]^2-\frac{1}{4}(\boldsymbol{d}-\boldsymbol{\xi})^4\right\} \\
&= 8\|g_{\varphi}\|^2\left\{\frac{1}{2}\left[\mathrm{Tr}\left(\Gamma-\frac{1}{2}\right)+\boldsymbol{d}^2\right]\right. \\
&\quad \left. +\frac{1}{4}\left[\mathrm{Tr}\left(\Gamma-\frac{1}{2}\right)+\boldsymbol{d}^2\right]^2-\frac{1}{4}[\mathrm{Tr}(\Gamma-\Gamma_0)+\boldsymbol{d}^2]^2\right\} \\
&= 8\|g_{\varphi}\|^2\left(\overline{N}(\overline{N}+1)-\frac{1}{4}[\mathrm{Tr}(\Gamma-\Gamma_0)+\boldsymbol{d}^2]^2\right) \\
&\leqslant 8\|g_{\varphi}\|^2\overline{N}(\overline{N}+1).
\end{aligned} \tag{3.37}$$

For the first equality, we have used the moments of the Gaussian distribution $P_{\Gamma}(\boldsymbol{\xi})$ in (3.33), i.e., $\int \mathrm{d}^{2M}\boldsymbol{\xi}\; P_{\Gamma}(\boldsymbol{\xi})\boldsymbol{\xi} = 0$ and $\int \mathrm{d}^{2M}\boldsymbol{\xi}\; P_{\Gamma}(\boldsymbol{\xi})\boldsymbol{\xi}^2 = \mathrm{Tr}(\Gamma - \Gamma_0)$. The inequality (3.37) proves that (1.4) holds irrespective of the purity of the input states. Furthermore, we notice that the last inequality is saturated if and only if

$$\mathrm{Tr}(\Gamma - \Gamma_0) = 0 \quad \text{and} \quad \boldsymbol{d} = 0. \tag{3.38}$$

Due to (3.35), the first condition requires

$$\Gamma = \Gamma_0, \tag{3.39}$$

implying that the only elements of $\mathcal{G}(M, \overline{N})$ which saturate the bound (1.4) are the pure ones, given in (3.31).

4. Measurements

In this section, we focus on the measurement $\mathcal{P}$ that attains the maximum on the right-hand side of (2.7) yielding the QFI. As it is the case for the optimal input state $|\psi_{\mathrm{opt}}\rangle$ analyzed in the previous section, we shall see that the optimal POVM also exhibits in general a nontrivial dependence on the target parameter φ, making it problematic to use it in realistic situations. Still, determining the optimal POVM explicitly is a well-defined problem which deserves to be addressed.

As a starting point of our study, we use the well-known fact that a POVM $\mathcal{P}$ that maximizes the FI of the problem can always be constructed by looking at the set of the eigenprojections of the SLD L_{φ} of the model [89]. We have given an SLD L_{φ} for a generic Gaussian state $\hat{\rho}_{\varphi}$ in (3.5), which for a pure Gaussian state reduces to (3.13). For our problem, in which the parameter φ is embedded in the probe state via a passive linear circuit, it reduces further to (3.15), which depends on the input state, i.e. its covariance matrix Γ and displacement $\boldsymbol{d}$, and the generator G_{φ} of the circuit. Specifying this expression in the case of the optimal input $|\psi_{\mathrm{opt}}\rangle$ in (3.31), we get

$$\hat{L}_{\varphi} = \mathrm{i}\varepsilon_1 \sinh 2r_0\, \hat{U}_{\varphi}\hat{V}_{\varphi}(\hat{a}_1^2 - \hat{a}_1^{\dagger 2})\hat{V}_{\varphi}^{\dagger}\hat{U}_{\varphi}^{\dagger}, \tag{4.1}$$

with $\hat{a}_1$ being the annihilation operator of the first probing mode, and ε_1 being the largest (in magnitude) eigenvalue of G_{φ}, which is put in the first mode after the diagonalization of G_{φ} by $\hat{V}_{\varphi}$ (see (A.21)–(A.24); recall also the discussion around (3.28)).

Notice, however, that SLD is not unique when the density operator $\hat{\rho}_{\varphi}$ is not of full rank: see (2.9). Indeed, there is a different and simple construction of SLD for a pure state. Since a pure state $\hat{\rho}_{\varphi}$ satisfies $\hat{\rho}_{\varphi} = \hat{\rho}_{\varphi}^2$, its derivative yields an SLD $\hat{L}_{\varphi}' = 2\mathrm{d}\hat{\rho}_{\varphi}/\mathrm{d}\varphi$, which for our problem with the optimal Gaussian input state $|\psi_{\mathrm{opt}}\rangle$ reads

$$\hat{L}_{\varphi}' = -2\mathrm{i}\hat{U}_{\varphi}[\hat{G}_{\varphi}, |\psi_{\mathrm{opt}}\rangle\langle\psi_{\mathrm{opt}}|]\hat{U}_{\varphi}^{\dagger}, \tag{4.2}$$

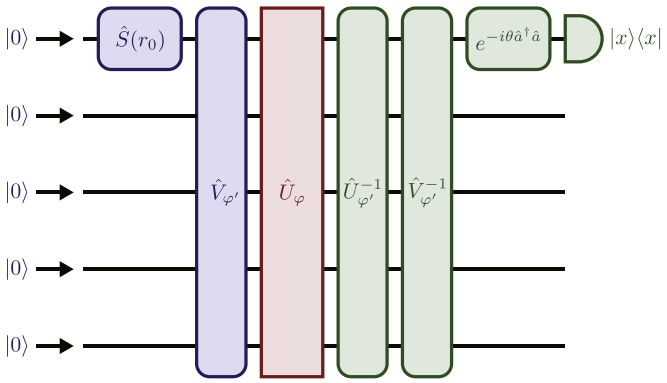

Figure 2. An overall circuit to achieve the ultimate precision bound in (1.4), including the preparation stage for the optimal input state $|\psi_{\rm opt}\rangle$ in (3.31) and the measurement stage, where $|x\rangle\langle x|$ represents the homodyne measurement on the first mode along the quadrature $\hat{x}_1 = (\hat{a}_1 + \hat{a}_1^\dagger)/\sqrt{2}$ and the phase shift θ is tuned to $\theta = \pm\tan^{-1}{\rm e}^{2r_0}$. Note that φ of $\hat{U}_\varphi$ is the target parameter to be estimated, which is not under our control, while φ' of $\hat{V}_{\varphi'}$, $\hat{U}_{\varphi'}^{-1}$, and $\hat{V}_{\varphi'}^{-1}$ is decided by ourselves. Tuning φ' to the true value φ provides us with the optimal strategy. The perfect cancellation of $\hat{U}_\varphi$ by $\hat{U}_{\varphi'}^{-1}$ tells us that our guessed value φ' perfectly matches the true value φ, and a small deviation can be sensitively detected by the strategy shown here with $\varphi' = \varphi$.

where

$$\hat{G}_\varphi = {\rm i}\hat{U}_\varphi^\dagger \frac{{\rm d}\hat{U}_\varphi}{{\rm d}\varphi} \tag{4.3}$$

is the generator of the target circuit $\hat{U}_\varphi$, which is quadratic in the canonical operators $\hat{\boldsymbol{a}}$ and $\hat{\boldsymbol{a}}^\dagger$. This SLD $\hat{L}'_\varphi$ is of rank 2, and its eigenbasis includes the two orthogonal eigenvectors

$$|\phi_\pm\rangle = \frac{1}{\sqrt{2}}\hat{U}_\varphi(|\psi_{\rm opt}\rangle \mp {\rm i}|\psi_{\rm opt}^\perp\rangle) \tag{4.4}$$

belonging to the two nonvanishing eigenvalues $\pm 2(\Delta G_\varphi)_{\rm opt}$, where

$$|\psi_{\rm opt}^\perp\rangle = \frac{1}{(\Delta G_\varphi)_{\rm opt}}(\hat{G}_\varphi - \langle\hat{G}_\varphi\rangle_{\rm opt})|\psi_{\rm opt}\rangle, \tag{4.5}$$

with $\langle\hat{G}_\varphi\rangle_{\rm opt} = \langle\psi_{\rm opt}|\,\hat{G}_\varphi|\psi_{\rm opt}\rangle$ and $(\Delta G_\varphi)^2_{\rm opt} = \langle\hat{G}_\varphi^2\rangle_{\rm opt} - \langle\hat{G}_\varphi\rangle^2_{\rm opt}$, is a state orthogonal to $|\psi_{\rm opt}\rangle$, i.e. $\langle\psi_{\rm opt}|\psi_{\rm opt}^\perp\rangle = 0$. Therefore, the measurement $\mathcal{P}$ with the POVM

$$\{|\phi_+\rangle\langle\phi_+|,\ |\phi_-\rangle\langle\phi_-|,\ \mathbb{I} - |\phi_+\rangle\langle\phi_+| - |\phi_-\rangle\langle\phi_-|\} \tag{4.6}$$

will achieve the upper bound of the QFI in (1.4). This is a generalization of the result given in [14], from a single-mode phase shift to a generic multimode passive linear circuit.

Another example of an optimal POVM can be obtained by considering the scheme depicted in figure 2 (the circuit in figure 2 includes both the preparation stage for the optimal input state $|\psi_{\rm opt}\rangle$ in (3.31) and the probing stage together with the circuit $\hat{U}_\varphi$). The measurement is to first undo the circuit $\hat{U}_\varphi$ as well as the transformation $\hat{V}_\varphi$ applied to prepare the optimal input state $|\psi_{\rm opt}\rangle$ in (3.31), and then to perform the homodyne measurement on the first mode along the quadrature $\hat{x}_1^{(\theta)} = {\rm e}^{{\rm i}\theta\hat{a}_1^\dagger\hat{a}_1}\hat{x}_1{\rm e}^{-{\rm i}\theta\hat{a}_1^\dagger\hat{a}_1} = \hat{x}_1\cos\theta + \hat{y}_1\sin\theta$ with $\theta = \pm\tan^{-1}{\rm e}^{2r_0}$. Accordingly, the elements $\{\hat{\Pi}_x\}$ of the POVM for this measurement can be expressed as

$$\hat{\Pi}_x = \hat{U}_\varphi\hat{V}_\varphi{\rm e}^{{\rm i}\theta\hat{a}_1^\dagger\hat{a}_1}(|x\rangle\langle x| \otimes \mathbb{I} \otimes \cdots \otimes \mathbb{I}){\rm e}^{-{\rm i}\theta\hat{a}_1^\dagger\hat{a}_1}\hat{V}_\varphi^\dagger\hat{U}_\varphi^\dagger, \tag{4.7}$$

where $|x\rangle$ is the eigenvector of the quadrature operator $\hat{x}_1$ such that $\hat{x}_1|x\rangle = x|x\rangle$, normalized as $\langle x|x'\rangle = \delta(x - x')$. Indeed, the FI by this POVM $\{\hat{\Pi}_x\}$ for the optimal input $|\psi_{\rm opt}\rangle$ in (3.31) coincides with the upper bound of the QFI in (1.4). See appendix D for the proof. This is a generalization of the result given in [19], from a single-mode phase shift to a generic multimode passive linear circuit.

5. Simple examples

Let us look at a few simple examples, i.e. the two- and three-mode circuits shown in figure 3, to see in particular how the unitary $\hat{V}_\varphi$ involved in the optimal input Gaussian state (3.31) looks like. The optimal input Gaussian states $|\psi_{\rm opt}\rangle$ and the maximal QFIs $F(\varphi||\psi_{\rm opt}\rangle)$ for those examples are summarized in table 1.

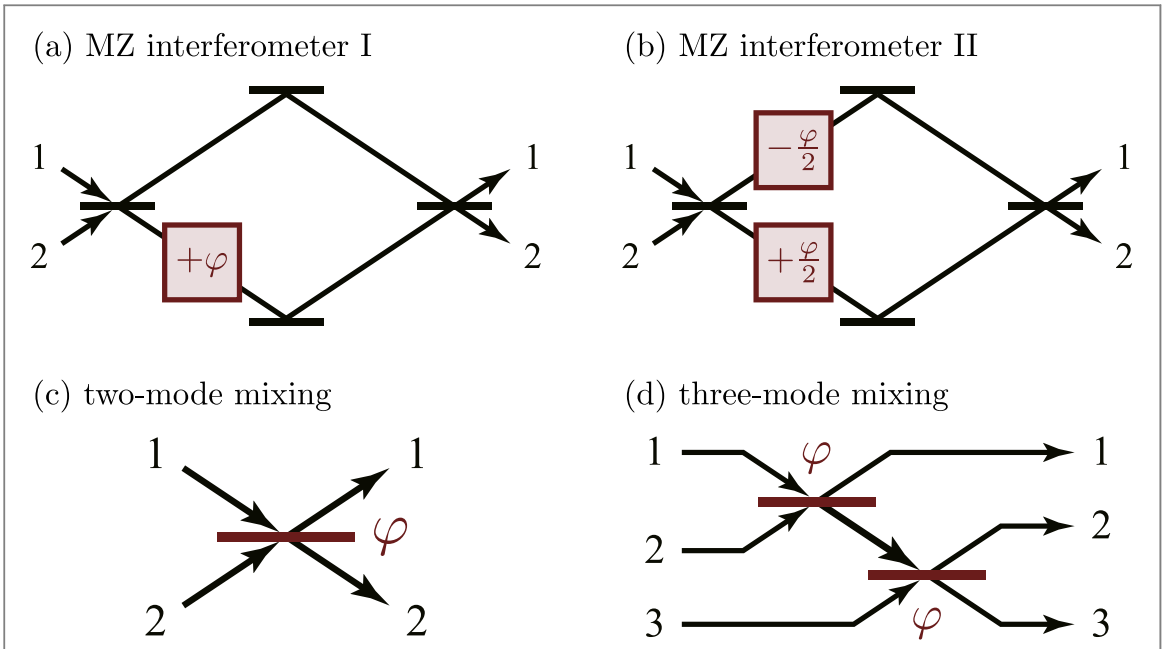

Figure 3. (a)–(b) Two different arrangements of the MZ interferometer. (c) Two-mode mixing circuit. (d) Three-mode mixing circuit.

Table 1. The optimal Gaussian input state $|\psi_{\rm opt}\rangle$ and the maximal QFI $F(\varphi||\psi_{\rm opt}\rangle)$ for the estimation of the parameter φ in each of the circuits shown in figure 3.

	$\|\psi_{\rm opt}\rangle$	$F(\varphi\|\|\psi_{\rm opt}\rangle)$
MZ interferometer I	$\hat{U}_{12}^{\dagger}\left(\frac{\pi}{4}\right)\hat{S}_1(r_0)\|0\rangle$	$8\overline{N}(\overline{N}+1)$
MZ interferometer II	$\hat{U}_{12}^{\dagger}\left(\frac{\pi}{4}\right)\hat{S}_1(r_0)\|0\rangle$	$2\overline{N}(\overline{N}+1)$
Two-mode mixing	$e^{\frac{\pi i}{4}(\hat{a}_1^{\dagger}\hat{a}_1-\hat{a}_2^{\dagger}\hat{a}_2)}\hat{U}_{12}^{\dagger}\left(\frac{\pi}{4}\right)\hat{S}_1(r_0)\|0\rangle$	$8\overline{N}(\overline{N}+1)$
Three-mode mixing	$\hat{U}_{12}^{\dagger}(\varphi)e^{\frac{\pi i}{2}\hat{a}_2^{\dagger}\hat{a}_2}\hat{U}_{31}\left(\frac{\pi}{4}\right)\hat{U}_{12}\left(\frac{\pi}{4}\right)\hat{S}_1(r_0)\|0\rangle$	$16\overline{N}(\overline{N}+1)$

5.1. Mach-Zehnder (MZ) interferometer I

We first consider the MZ interferometer in figure 3(a). Our target is the phase shift φ in one of the two arms of the interferometer. The state of the probe photons going through this MZ interferometer is transformed by the unitary transformation

$$\hat{U}_{\varphi}=\hat{U}_{12}^{\dagger}\left(\frac{\pi}{4}\right)e^{-i\varphi\hat{a}_1^{\dagger}\hat{a}_1}\hat{U}_{12}\left(\frac{\pi}{4}\right), \tag{5.1}$$

where

$$\hat{U}_{mn}(\theta)=e^{\theta(\hat{a}_n^{\dagger}\hat{a}_m-\hat{a}_m^{\dagger}\hat{a}_n)} \tag{5.2}$$

describes a beam splitter for modes m and n, which acts on the canonical operators as

$$\begin{pmatrix}\hat{U}_{mn}^{\dagger}(\theta)\hat{a}_m\hat{U}_{mn}(\theta)\\ \hat{U}_{mn}^{\dagger}(\theta)\hat{a}_n\hat{U}_{mn}(\theta)\end{pmatrix}=\begin{pmatrix}\cos\theta & -\sin\theta\\ \sin\theta & \cos\theta\end{pmatrix}\begin{pmatrix}\hat{a}_m\\ \hat{a}_n\end{pmatrix}=U_{mn}(\theta)\begin{pmatrix}\hat{a}_m\\ \hat{a}_n\end{pmatrix}, \tag{5.3}$$

with θ characterizing its transmissivity. In particular, $\hat{U}_{mn}\left(\frac{\pi}{4}\right)$ describes a balanced beam splitter. The generator of this two-mode circuit reads

$$\hat{G}_{\varphi}=i\hat{U}_{\varphi}^{\dagger}\frac{d\hat{U}_{\varphi}}{d\varphi}=\hat{U}_{12}^{\dagger}\left(\frac{\pi}{4}\right)\hat{a}_1^{\dagger}\hat{a}_1\hat{U}_{12}\left(\frac{\pi}{4}\right). \tag{5.4}$$

The unitary matrix U_{φ} related to the unitary transformation $\hat{U}_{\varphi}$ through (2.2) is given by

$$U_{\varphi}=U_{12}^{\dagger}\left(\frac{\pi}{4}\right)\begin{pmatrix}e^{-i\varphi} & 0\\ 0 & 1\end{pmatrix}U_{12}\left(\frac{\pi}{4}\right), \tag{5.5}$$

and its generator reads

$$g_\varphi = \mathrm{i}U_\varphi^\dagger \frac{\mathrm{d}U_\varphi}{\mathrm{d}\varphi} = U_{12}^\dagger\left(\frac{\pi}{4}\right)\begin{pmatrix}1 & 0\\ 0 & 0\end{pmatrix}U_{12}\left(\frac{\pi}{4}\right). \tag{5.6}$$

We thus have

$$\|g_\varphi\| = 1. \tag{5.7}$$

The unitary operator $\hat{V}_\varphi$ corresponding to the unitary matrix diagonalizing g_φ in (5.6) (compare it with (A.23)) is

$$\hat{V}_\varphi = \hat{U}_{12}^\dagger\left(\frac{\pi}{4}\right). \tag{5.8}$$

Therefore, the optimal Gaussian input state (3.31) for this MZ interferometer is given by

$$|\psi_{\mathrm{opt}}\rangle = \hat{U}_{12}^\dagger\left(\frac{\pi}{4}\right)\hat{S}_1(r_0)|0\rangle, \tag{5.9}$$

with the squeezing parameter r_0 given in (3.30). By this choice, the QFI reaches the upper bound in (1.4), yielding

$$F(\varphi||\psi_{\mathrm{opt}}\rangle) = 8\overline{N}(\overline{N}+1). \tag{5.10}$$

Notice that, in this case, the optimal input state $|\psi_{\mathrm{opt}}\rangle$ in (5.9) is *independent* of the target parameter φ. Note also that the same expression as (5.10) is found e.g. in [14, 19, 34, 40, 59], but it is found there as the optimal QFI for the estimation of the *single-mode* phase shift with a Gaussian probe. Here, (5.10) is presented as the optimal QFI for the *two-mode* circuit in figure 3(a).

The unitary transformation $\hat{U}_{12}^\dagger\left(\frac{\pi}{4}\right)$ in the optimal input state (5.9) 'unfolds' the first beam splitter $\hat{U}_{12}\left(\frac{\pi}{4}\right)$ of the MZ interferometer. Thus, the best strategy effectively consists in sending the single-mode squeezed vacuum $|r_0\rangle = \hat{S}_1(r_0)|0\rangle$ directly to the phase shifter without the first beam splitter $\hat{U}_{12}\left(\frac{\pi}{4}\right)$. The second beam splitter $\hat{U}_{12}^\dagger\left(\frac{\pi}{4}\right)$ of the MZ interferometer is also unfolded by $\hat{U}_{12}\left(\frac{\pi}{4}\right)$ performed in the optimal measurements (see (4.4) and (4.7), where $\hat{U}_\varphi$ contains $\hat{U}_{12}^\dagger\left(\frac{\pi}{4}\right)$, whose Hermitian conjugate $\hat{U}_{12}\left(\frac{\pi}{4}\right)$ in $\hat{U}_\varphi^\dagger$ acts on the output probe state first in the measurement process, canceling the second beam splitter $\hat{U}_{12}^\dagger\left(\frac{\pi}{4}\right)$).

5.2. MZ interferometer II

Let us look at the MZ interferometer in the slightly different configuration shown in figure 3(b). This setup induces the unitary transformation

$$\hat{U}_\varphi = \hat{U}_{12}^\dagger\left(\frac{\pi}{4}\right)\mathrm{e}^{-\mathrm{i}\frac{\varphi}{2}(\hat{a}_1^\dagger\hat{a}_1-\hat{a}_2^\dagger\hat{a}_2)}\hat{U}_{12}\left(\frac{\pi}{4}\right), \tag{5.11}$$

and its generator is given by

$$\hat{G}_\varphi = \frac{1}{2}\hat{U}_{12}^\dagger\left(\frac{\pi}{4}\right)(\hat{a}_1^\dagger\hat{a}_1 - \hat{a}_2^\dagger\hat{a}_2)\hat{U}_{12}\left(\frac{\pi}{4}\right). \tag{5.12}$$

The unitary matrix U_φ corresponding to the unitary operator $\hat{U}_\varphi$ in (5.11) is given by

$$U_\varphi = U_{12}^\dagger\left(\frac{\pi}{4}\right)\begin{pmatrix}\mathrm{e}^{-\mathrm{i}\varphi/2} & 0\\ 0 & \mathrm{e}^{\mathrm{i}\varphi/2}\end{pmatrix}U_{12}\left(\frac{\pi}{4}\right), \tag{5.13}$$

while the Hermitian matrix g_φ corresponding to the generator $\hat{G}_\varphi$ in (5.12) reads

$$g_\varphi = U_{12}^\dagger\left(\frac{\pi}{4}\right)\begin{pmatrix}1/2 & 0\\ 0 & -1/2\end{pmatrix}U_{12}\left(\frac{\pi}{4}\right). \tag{5.14}$$

We thus have

$$\|g_\varphi\| = \frac{1}{2}. \tag{5.15}$$

The optimal Gaussian input state for this MZ interferometer is the same as the one given in (5.9), while the maximal QFI achievable by the optimal input state is

$$F(\varphi||\psi_{\mathrm{opt}}\rangle) = 2\overline{N}(\overline{N}+1). \tag{5.16}$$

This QFI is lower than the previous one in (5.10) for the other MZ interferometer, even though the relative phases φ to be estimated in the two MZ interferometers are the same. This is because injecting all the resources to one of the two arms of the interferometer is optimal if we stick to Gaussian probes, and only one of the two phase shifters in figure 3(b) is probed. It would be worth noticing that our estimation problem implicitly assumes the presence of an external phase reference. Without the reference beam, the two MZ interferometers in figures 3(a)

and (b) are equivalent, since only the relative phase between the two arms matters in such a case. See the discussion in [26].

5.3. Two-mode mixing

Let us look at another two-mode example: the estimation of the parameter φ characterizing the transmissivity of the beam splitter represented by the unitary transformation

$$\hat{U}_\varphi = \hat{U}_{12}(\varphi). \tag{5.17}$$

See figure 3(c). Its generator reads

$$\hat{G}_\varphi = \mathrm{i}(\hat{a}_2^\dagger \hat{a}_1 - \hat{a}_1^\dagger \hat{a}_2), \tag{5.18}$$

which can be rewritten as

$$\hat{G}_\varphi = \mathrm{e}^{\frac{\pi \mathrm{i}}{4}(\hat{a}_1^\dagger \hat{a}_1 - \hat{a}_2^\dagger \hat{a}_2)} \hat{U}_{12}^\dagger\left(\tfrac{\pi}{4}\right)(\hat{a}_1^\dagger \hat{a}_1 - \hat{a}_2^\dagger \hat{a}_2)\, \hat{U}_{12}\left(\tfrac{\pi}{4}\right)\mathrm{e}^{-\frac{\pi \mathrm{i}}{4}(\hat{a}_1^\dagger \hat{a}_1 - \hat{a}_2^\dagger \hat{a}_2)}. \tag{5.19}$$

It is unitarily equivalent to the generator $\hat{G}_\varphi$ in (5.12), apart from the numerical proportionality constant $1/2$. We thus have

$$\|g_\varphi\| = 1, \tag{5.20}$$

and the maximal QFI is given by

$$F(\varphi||\psi_{\mathrm{opt}}\rangle) = 8\overline{N}(\overline{N}+1). \tag{5.21}$$

This is reached by the input state

$$|\psi_{\mathrm{opt}}\rangle = \mathrm{e}^{\frac{\pi \mathrm{i}}{4}(\hat{a}_1^\dagger \hat{a}_1 - \hat{a}_2^\dagger \hat{a}_2)} \hat{U}_{12}^\dagger\left(\tfrac{\pi}{4}\right)\hat{S}_1(r_0)|0\rangle, \tag{5.22}$$

with the squeezing parameter r_0 given in (3.30). This optimal state is again independent of the target parameter φ.

The same estimation problem, i.e. the estimation of φ in the two-mode mixing channel (5.17), is studied in [59], but the maximal QFI (5.21) and the optimal Gaussian input state (5.22) are not identified there.

5.4. Three-mode mixing

Let us also look at a three-mode example. We consider the circuit shown in figure 3(d), composed of two beam splitters of the same transmissivity characterized by the parameter φ. Our problem is to estimate the single parameter φ in the three-mode mixing circuit represented by the unitary transformation

$$\hat{U}_\varphi = \hat{U}_{23}(\varphi)\hat{U}_{12}(\varphi). \tag{5.23}$$

Its generator reads

$$\begin{aligned}\hat{G}_\varphi &= \mathrm{i}\hat{U}_{12}^\dagger(\varphi)(\hat{a}_3^\dagger \hat{a}_2 - \hat{a}_2^\dagger \hat{a}_3 + \hat{a}_2^\dagger \hat{a}_1 - \hat{a}_1^\dagger \hat{a}_2)\hat{U}_{12}(\varphi) \\ &= \sqrt{2}\ \hat{V}_\varphi(\hat{a}_1^\dagger \hat{a}_1 - \hat{a}_2^\dagger \hat{a}_2)\hat{V}_\varphi^\dagger,\end{aligned} \tag{5.24}$$

with

$$\hat{V}_\varphi = \hat{U}_{12}^\dagger(\varphi)\mathrm{e}^{\frac{\pi \mathrm{i}}{2}\hat{a}_2^\dagger \hat{a}_2}\hat{U}_{31}\left(\tfrac{\pi}{4}\right)\hat{U}_{12}\left(\tfrac{\pi}{4}\right). \tag{5.25}$$

We have

$$\|g_\varphi\| = \sqrt{2}, \tag{5.26}$$

and the maximal QFI is given by

$$F(\varphi||\psi_{\mathrm{opt}}\rangle) = 16\overline{N}(\overline{N}+1). \tag{5.27}$$

This is reached by the input state

$$|\psi_{\mathrm{opt}}\rangle = \hat{U}_{12}^\dagger(\varphi)\mathrm{e}^{\frac{\pi \mathrm{i}}{2}\hat{a}_2^\dagger \hat{a}_2}\hat{U}_{31}\left(\tfrac{\pi}{4}\right)\hat{U}_{12}\left(\tfrac{\pi}{4}\right)\hat{S}_1(r_0)|0\rangle, \tag{5.28}$$

with the squeezing parameter r_0 given in (3.30). In this case, the optimal input state depends on the target parameter φ.

If our guess φ' is not precise and does not match the true value φ, the input state (3.31) and the measurement, e.g. (4.6) or (4.7), prepared and performed with the guessed value φ' in place of φ (see e.g. the circuit in figure 2) are not optimal, and the FI for such a nonoptimal probing deviates from the maximal QFI in (1.4). Since we assume that the functional dependence of $\hat{U}_\varphi$ upon φ is smooth, the FI is a smooth function of φ', and therefore, the deviation of FI from the maximal QFI is only quadratic around the optimal point $\varphi' = \varphi$. In this sense, the FI is robust to a small error in the guess of φ.

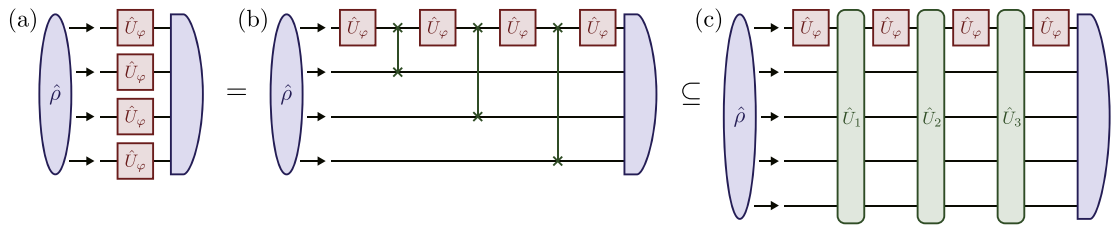

Figure 4. The parallel scheme in (a) is equivalent to the sequential scheme in (b) with the target circuits $\hat{U}_\varphi$ swapped by SWAP gates, which is a particular case of the sequential scheme in (c) with generic gates $\hat{U}_\ell$ entangling the main probes with additional ancillas.

6. Sequential strategy

If we are allowed to use multiple (identical) target circuits $\hat{U}_\varphi$ at the same time, we could do better. Suppose that we are given L identical M-mode passive linear circuits $\hat{U}_\varphi$. A paradigmatic scheme for the quantum metrology is the parallel scheme in figure 4(a) with an entangled input $\hat{\rho}$ [2, 4]. The result in section 3 suggests, however, that, if we stick to Gaussian inputs, this parallel setup does not help improve the maximal QFI found in (1.4), since the best strategy is to inject all the resources into a single-mode of the overall LM-mode passive linear circuit in figure 4(a): only one of the L circuits is probed with the others irrelevant. See (3.31). On the other hand, if we are allowed to perform some operations $\{\hat{U}_1, \ldots, \hat{U}_{L-1}\}$ between the target gates $\hat{U}_\varphi$ with ancilla modes introduced as in figure 4(c), we can hope to do better. Let us restrict ourselves to passive linear controls $\{\hat{U}_1, \ldots, \hat{U}_{L-1}\}$, and seek for the optimal strategy with a Gaussian input $\hat{\rho} \in \mathcal{G}(K, \overline{N})$, where $K \geqslant LM$.

The circuit in figure 4(c) is described by the unitary

$$\hat{\mathcal{U}}_\varphi = \hat{U}_\varphi \hat{U}_{L-1} \hat{U}_\varphi \cdots \hat{U}_2 \hat{U}_\varphi \hat{U}_1 \hat{U}_\varphi. \tag{6.1}$$

Note that there are $K\,(\geqslant LM)$ modes in total in the overall circuit, and the unitary operators $\hat{U}_\varphi$ act only on the first M modes, i.e. $\hat{U}_\varphi \otimes \mathbb{I}$. By abuse of notation, $\hat{U}_\varphi \otimes \mathbb{I}$ is simply denoted by $\hat{U}_\varphi$ in (6.1). The overall circuit is a K-mode passive linear circuit, and the orthogonal matrix $\mathcal{R}_\varphi$ which rotates the quadrature operators $\hat{\boldsymbol{z}}$ in phase space according to the transformation $\hat{\mathcal{U}}_\varphi$ is given by

$$\mathcal{R}_\varphi = W^\dagger \begin{pmatrix} \mathcal{U}_\varphi & 0 \\ 0 & \mathcal{U}_\varphi^* \end{pmatrix} W \tag{6.2}$$

with

$$\mathcal{U}_\varphi = U_\varphi U_{L-1} U_\varphi \cdots U_2 U_\varphi U_1 U_\varphi, \tag{6.3}$$

where U_φ and U_ℓ ($\ell = 1, \ldots, L-1$) are $K \times K$ unitary matrices corresponding to $\hat{U}_\varphi \otimes \mathbb{I}$ and $\hat{U}_\ell$, respectively. The quantity relevant to the maximal QFI is the spectral norm of the generator of this orthogonal transformation $\mathcal{R}_\varphi$ (see (1.4)), i.e. the largest (in magnitude) eigenvalue of

$$\mathcal{G}_\varphi = \mathrm{i}\mathcal{U}_\varphi^\dagger \frac{\mathrm{d}\mathcal{U}_\varphi}{\mathrm{d}\varphi} = \sum_{\ell=0}^{L-1} U_\varphi^\dagger U_1^\dagger \cdots U_\varphi^\dagger U_\ell^\dagger g_\varphi U_\ell U_\varphi \cdots U_1 U_\varphi, \tag{6.4}$$

where

$$g_\varphi = \mathrm{i} U_\varphi^\dagger \frac{\mathrm{d}U_\varphi}{\mathrm{d}\varphi}. \tag{6.5}$$

The spectral norm of the generator $\mathcal{G}_\varphi$ is bounded from above as

$$\begin{aligned} \|\mathcal{G}_\varphi\| &= \left\| \sum_{\ell=0}^{L-1} U_\varphi^\dagger U_1^\dagger \cdots U_\varphi^\dagger U_\ell^\dagger g_\varphi U_\ell U_\varphi \cdots U_1 U_\varphi \right\| \\ &\leqslant \sum_{\ell=0}^{L-1} \| U_\varphi^\dagger U_1^\dagger \cdots U_\varphi^\dagger U_\ell^\dagger g_\varphi U_\ell U_\varphi \cdots U_1 U_\varphi \| = L \|g_\varphi\|. \end{aligned} \tag{6.6}$$

This inequality is saturated if

$$[g_\varphi, U_\ell U_\varphi] = 0 \qquad (\ell = 1, \ldots, L-1). \tag{6.7}$$

A sufficient and general solution is given by

$$U_\ell = U_\varphi^\dagger \qquad (\ell = 1, \ldots, L-1) \tag{6.8}$$

(see [95]). By this choice, the generator of the overall circuit $\hat{\mathcal{U}}_\varphi$ is reduced to $\mathcal{G}_\varphi = Lg_\varphi$, and the upper bound on the QFI by the sequential strategy with a Gaussian input $\hat{\rho} \in \mathcal{G}(K, \overline{N})$ is given by

$$\mathcal{F}(\varphi|\hat{\rho}) \leqslant 8L^2\|g_\varphi\|^2\overline{N}(\overline{N}+1). \tag{6.9}$$

This upper bound is saturated by the input state

$$|\Psi_{\rm opt}\rangle = |\psi_{\rm opt}\rangle \otimes |0\rangle, \tag{6.10}$$

with $|\psi_{\rm opt}\rangle$ given in (3.31) for the first M modes while vacuum for the rest.

The results in (6.8) and (6.10) show that the ancilla modes are not necessary for the optimal strategy. We note that in general the optimal controls (6.8) and the optimal input state (6.10) depend on the target parameter φ.

7. Summary

We have clarified the universal bound (1.4) on the precision of the estimation (QFI) of a parameter embedded in a generic multimode passive (photon number preserving) linear optical circuit by using Gaussian probes with a given average number of probe photons $\overline{N}$. We have identified the input Gaussian state (3.31) that yields the QFI saturating the bound (1.4): it is a single-mode squeezed vacuum in an appropriate basis. We have also found measurements (POVMs) (4.6) and (4.7) by which FI reaches QFI. The best (sequential) strategy when we are given multiple identical target circuits and are allowed to apply passive linear controls in between with the help of an arbitrary number of ancilla modes has been revealed: no ancilla mode is actually needed for the best strategy[6].

Even though the optimal input state (3.31) and the optimal measurements (4.6) and (4.7), as well as the optimal controls (6.8) in the sequential strategy, depend on the target parameter to be estimated in general and adaptive adjustments of the input, the measurement, and the controls would be required to achieve the precision bound in practice, the above result shows that the bound is sharp and covers various specific setups composed of phase shifters and beam splitters, including the standard MZ interferometer, providing the universal bound that cannot be beaten by any Gaussian inputs and any passive controls.

The present work has focussed on passive linear circuits. Bounds on more general Gaussian metrology, for general Gaussian channels including amplitude-damping channels and channels involving squeezing, etc., have not been thoroughly understood yet, beyond analyses on specific setups. Entanglement with ancilla modes would be useful for such generic Gaussian metrology [17] and it would be interesting to explore.

Acknowledgments

KY thanks Koji Matsuoka for the discussions during his master's thesis study [98], in which the bound (1.4) and the optimal input state (3.31) were found for some restricted setups. This work was supported by the Top Global University Project from the Ministry of Education, Culture, Sports, Science and Technology (MEXT), Japan. KY was supported by the Grant-in-Aid for Scientific Research (C) (No.18K03470) from the Japan Society for the Promotion of Science (JSPS) and by the Waseda University Grant for Special Research Projects (No. 2018K-262). PF was supported by INFN through the project 'QUANTUM,' and by the Italian National Group of Mathematical Physics (GNFM-INdAM).

Appendix A. Gaussian states and operations

In order to introduce a proper definition of the Gaussian set $\mathcal{G}(M, \overline{N})$, we find it useful to introduce the quadrature operators $\hat{x}_m$ and $\hat{y}_m$ for each of the M modes,

$$\begin{cases} \hat{x}_m = \frac{\hat{a}_m + \hat{a}_m^\dagger}{\sqrt{2}} \\ \hat{y}_m = \frac{\hat{a}_m - \hat{a}_m^\dagger}{\sqrt{2}\,\mathrm{i}} \end{cases} \qquad (m = 1, \ldots, M). \tag{A.1}$$

[6] There are works in the literature which discuss the unnecessity of mode entanglement [5, 39, 40, 50, 53, 55, 96, 97]. Note, however, that in those works the probe states are not restricted to Gaussian states and in addition just the achievability of the Heisenberg scaling (quadratic in $\overline{N}$) is discussed. The chosen probe states are not necessarily the optimal ones, even though they actually yields QFIs scaling quadratically in $\overline{N}$ (their coefficients are not necessarily the optimal). On the other hand, in the present work, we look at the optimal state which yields the maximal QFI.

Aligning these operators as a column vector

$$\hat{\boldsymbol{z}} = \begin{pmatrix} \hat{\boldsymbol{x}} \\ \hat{\boldsymbol{y}} \end{pmatrix} = \begin{pmatrix} \hat{x}_1 \\ \vdots \\ \hat{x}_M \\ \hat{y}_1 \\ \vdots \\ \hat{y}_M \end{pmatrix}, \tag{A.2}$$

the above relation (A.1) can be expressed as

$$\begin{pmatrix} \hat{\boldsymbol{a}} \\ \hat{\boldsymbol{a}}^\dagger \end{pmatrix} = W \begin{pmatrix} \hat{\boldsymbol{x}} \\ \hat{\boldsymbol{y}} \end{pmatrix} \tag{A.3}$$

with a $2M \times 2M$ unitary matrix

$$W = \frac{1}{\sqrt{2}} \begin{pmatrix} \mathbb{I} & \mathrm{i}\mathbb{I} \\ \mathbb{I} & -\mathrm{i}\mathbb{I} \end{pmatrix}. \tag{A.4}$$

The canonical commutation relations (2.1) can then be expressed in the compact form

$$[\hat{z}_m, \hat{z}_n] = \mathrm{i}J_{mn} \qquad (m, n = 1, \ldots, 2M), \tag{A.5}$$

with J being the $2M \times 2M$ real matrix

$$J = \begin{pmatrix} 0 & \mathbb{I} \\ -\mathbb{I} & 0 \end{pmatrix}. \tag{A.6}$$

A.1. Gaussian states

A Gaussian state $\hat{\rho}$ is fully characterized by its covariance matrix Γ and its displacement $\boldsymbol{d}$, defined by

$$\Gamma_{mn} = \frac{1}{2}\langle\{\hat{z}_m, \hat{z}_n\}\rangle - \langle\hat{z}_m\rangle\langle\hat{z}_n\rangle, \quad d_m = \langle\hat{z}_m\rangle \quad (m, n = 1, \ldots, 2M), \tag{A.7}$$

where $\langle\cdots\rangle$ denotes the expectation value on $\hat{\rho}$. In particular, its characteristic function reads as

$$\chi(\boldsymbol{\eta}) = \langle \mathrm{e}^{\mathrm{i}\boldsymbol{\eta}\cdot\hat{\boldsymbol{z}}}\rangle = \mathrm{e}^{-\frac{1}{2}\boldsymbol{\eta}^T\Gamma\boldsymbol{\eta} + \mathrm{i}\boldsymbol{\eta}\cdot\boldsymbol{d}}. \tag{A.8}$$

Furthermore, $\hat{\rho}$ is an element of $\mathcal{G}(M, \overline{N})$ when its mean photon number is equal to $\overline{N}$, i.e.

$$\langle\hat{N}\rangle = \frac{1}{2}\left[\mathrm{Tr}\left(\Gamma - \frac{1}{2}\right) + \boldsymbol{d}^2\right] = \overline{N}, \tag{A.9}$$

where the number operator $\hat{N}$ is defined in (2.3). The covariance matrix Γ is real, symmetric, and positive-definite, and hence, according to Williamson's theorem it admits the canonical decomposition [83, 84]

$$\Gamma = RQR'\Sigma R'^T Q R^T, \tag{A.10}$$

where

$$\Sigma = \begin{pmatrix} \sigma & 0 \\ 0 & \sigma \end{pmatrix}, \qquad Q = \begin{pmatrix} \mathrm{e}^{r} & 0 \\ 0 & \mathrm{e}^{-r} \end{pmatrix}, \tag{A.11}$$

$$R = W^\dagger \begin{pmatrix} U & 0 \\ 0 & U* \end{pmatrix} W, \qquad R' = W^\dagger \begin{pmatrix} U' & 0 \\ 0 & U'* \end{pmatrix} W, \tag{A.12}$$

with $M \times M$ diagonal submatrices

$$\sigma = \begin{pmatrix} \sigma_1 & & \\ & \ddots & \\ & & \sigma_M \end{pmatrix}, \qquad r = \begin{pmatrix} r_1 & & \\ & \ddots & \\ & & r_M \end{pmatrix}, \tag{A.13}$$

and $M \times M$ unitary submatrices U and U'[7]. The $2M \times 2M$ matrices R and R' are real orthogonal matrices, and we have $R^T = R^\dagger = R^{-1}$ and $R'^T = R'^\dagger = R'^{-1}$. The parameters $\{\sigma_1, \ldots, \sigma_M\}$ are the symplectic eigenvalues of Γ, which control the purity $p(\hat{\rho})$ of the Gaussian state $\hat{\rho}$ through [84]

[7] Note that U^* is not the Hermitian conjugate $U^\dagger$ of the $M \times M$ matrix U, but is obtained by taking the complex conjugate of each matrix element of U. In other words, it is $U* = (U^\dagger)^T = (U^T)^\dagger$, with T denoting the matrix transpose. This U^* is necessary in the structure of R in (A.12), for the symplectic character of R.

$$p(\hat{\rho}) = \mathrm{Tr}\,\hat{\rho}^2 = \frac{1}{\sqrt{\det(2\Gamma)}} = \prod_{m=1}^{M} \frac{1}{2\sigma_m}, \tag{A.14}$$

while $\{r_1, \ldots, r_M\}$ are the squeezing parameters. The symplectic eigenvalues are bounded from below by $\sigma_m \geqslant 1/2$ $(m = 1, \ldots, M)$ due to the uncertainty principle [83, 84]. The Gaussian state $\hat{\rho}$ is pure, $p(\hat{\rho}) = 1$, if and only if all the symplectic eigenvalues saturate the lower bounds $\sigma_m = 1/2$ $(m = 1, \ldots, M)$. Without loss of generality, we assume that

$$\sigma_1 \geqslant \sigma_2 \geqslant \cdots \geqslant \sigma_M \geqslant \frac{1}{2}, \qquad r_1 \geqslant r_2 \geqslant \cdots \geqslant r_M \geqslant 0. \tag{A.15}$$

This reordering can always be done by arranging properly R and R'. The matrices R and R' are symplectic and orthogonal, characterized by the structure (A.12) with the unitary matrices U and U'. The squeezing matrix Q is also symplectic. The symplectic character of these matrices is characterized by

$$R^T J R = J, \qquad R'^T J R' = J, \qquad Q^T J Q = J. \tag{A.16}$$

A.2. *M*-mode passive Gaussian unitary

Our target circuit $\hat{U}_\varphi$ is a generic M-mode passive Gaussian unitary, whose action is characterized by the $M \times M$ unitary matrix U_φ introduced in (2.2). In terms of the quadrature operators $\hat{z}_m$, it is rephrased as

$$\hat{U}_\varphi^\dagger \hat{z}_m \hat{U}_\varphi = \sum_{n=1}^{2M} (R_\varphi)_{mn} \hat{z}_n \qquad (m = 1, \ldots, 2M), \tag{A.17}$$

or simply written as $\hat{U}_\varphi^\dagger \hat{\boldsymbol{z}} \hat{U}_\varphi = R_\varphi \hat{\boldsymbol{z}}$, with R_φ being the $2M \times 2M$ orthogonal matrix defined by

$$R_\varphi = W^\dagger \begin{pmatrix} U_\varphi & 0 \\ 0 & U_\varphi^* \end{pmatrix} W. \tag{A.18}$$

As is clear from this structure, the matrix R_φ is symplectic and orthogonal, and the passive linear transformation $\hat{U}_\varphi$ is a rotation on the phase space.

By construction the transformation $\hat{U}_\varphi$ maps the set $\mathcal{G}(M, \overline{N})$ into itself. In particular, given $\hat{\rho} \in \mathcal{G}(M, \overline{N})$, the covariance matrix Γ_φ and the displacement $\boldsymbol{d}_\varphi$ of the associated Gaussian output state $\hat{\rho}_\varphi$ in (1.1) are obtained by rotating the covariance matrix Γ and the displacement $\boldsymbol{d}$ of the input state $\hat{\rho}$ as

$$\Gamma_\varphi = R_\varphi \Gamma R_\varphi^T, \qquad \boldsymbol{d}_\varphi = R_\varphi \boldsymbol{d}. \tag{A.19}$$

Note that they still fulfill the constraint (A.9) due to the fact that R_φ is orthogonal.

An important role on our problem is played by the generator of the transformation $\hat{U}_\varphi$, i.e. by the operator

$$\hat{G}_\varphi = \mathrm{i} \hat{U}_\varphi^\dagger \frac{\mathrm{d}\hat{U}_\varphi}{\mathrm{d}\varphi}, \tag{A.20}$$

whose equivalent on the phase space reads

$$G_\varphi = \mathrm{i} R_\varphi^T \frac{\mathrm{d}R_\varphi}{\mathrm{d}\varphi} = W^\dagger \begin{pmatrix} g_\varphi & 0 \\ 0 & -g_\varphi^* \end{pmatrix} W \tag{A.21}$$

with

$$g_\varphi = \mathrm{i} U_\varphi^\dagger \frac{\mathrm{d}U_\varphi}{\mathrm{d}\varphi}. \tag{A.22}$$

This g_φ is an $M \times M$ Hermitian matrix, that can be diagonalized by means of an $M \times M$ unitary matrix V_φ,

$$g_\varphi = V_\varphi \varepsilon_\varphi V_\varphi^\dagger, \qquad \varepsilon_\varphi = \begin{pmatrix} \varepsilon_1 & & \\ & \ddots & \\ & & \varepsilon_M \end{pmatrix}, \tag{A.23}$$

where, without loss of generality, the magnitudes of the eigenvalues ε_m of g_φ are ordered in decreasing order

$$|\varepsilon_1| \geqslant |\varepsilon_2| \geqslant \cdots \geqslant |\varepsilon_M|. \tag{A.24}$$

The generator G_φ is accordingly diagonalized as

$$G_\varphi = P_\varphi W^\dagger \begin{pmatrix} \varepsilon_\varphi & 0 \\ 0 & -\varepsilon_\varphi \end{pmatrix} W P_\varphi^T = P_\varphi (\mathcal{E}_\varphi \mathrm{i} J) P_\varphi^T, \tag{A.25}$$

where

$$P_\varphi = W^\dagger \begin{pmatrix} V_\varphi & 0 \\ 0 & V_\varphi^* \end{pmatrix} W, \qquad \mathcal{E}_\varphi = \begin{pmatrix} \varepsilon_\varphi & 0 \\ 0 & \varepsilon_\varphi \end{pmatrix}. \tag{A.26}$$

Appendix B. Derivation of the expression (3.17) for $F^{(1)}(\varphi|\hat{\rho})$

Here, we show the derivation of the expression for $F^{(1)}(\varphi|\hat{\rho})$ in (3.17). Notice first that R in (A.12) is a real matrix, and hence,

$$R^T = R^\dagger = R^{-1} = W^\dagger \begin{pmatrix} U^\dagger & 0 \\ 0 & U^T \end{pmatrix} W. \tag{B.1}$$

Inserting this into (3.9), the covariance matrix Γ of a pure Gaussian state is expressed as

$$\begin{aligned} \Gamma &= \frac{1}{2} W^\dagger \begin{pmatrix} U & 0 \\ 0 & U^* \end{pmatrix} W \begin{pmatrix} \mathrm{e}^{2r} & 0 \\ 0 & \mathrm{e}^{-2r} \end{pmatrix} W^\dagger \begin{pmatrix} U^\dagger & 0 \\ 0 & U^T \end{pmatrix} W \\ &= \frac{1}{2} W^\dagger \begin{pmatrix} U \cosh 2r\ U^\dagger & U \sinh 2r\ U^T \\ U^* \sinh 2r\ U^\dagger & U^* \cosh 2r\ U^T \end{pmatrix} W, \end{aligned} \tag{B.2}$$

and we have

$$\Gamma^{-1} = 2W^\dagger \begin{pmatrix} U \cosh 2r\ U^\dagger & -U \sinh 2r\ U^T \\ -U^* \sinh 2r\ U^\dagger & U^* \cosh 2r\ U^T \end{pmatrix} W. \tag{B.3}$$

Then, inserting these and (A.21) into the first line of (3.17), we get

$$\begin{aligned} F^{(1)}(\varphi|\hat{\rho}) &= \frac{1}{2} \mathrm{Tr}(G_\varphi \Gamma^{-1} G_\varphi \Gamma - G_\varphi^2) \\ &= \frac{1}{2} \mathrm{Tr}[(U^\dagger g_\varphi U \cosh 2r)^2] + \frac{1}{2} \mathrm{Tr}[(\cosh 2r\ U^T g_\varphi^* U^*)^2] \\ &\quad + \mathrm{Tr}(U^\dagger g_\varphi U \sinh 2r\ U^T g_\varphi^* U^* \sinh 2r) - \frac{1}{2} \mathrm{Tr}(g_\varphi^2) - \frac{1}{2} \mathrm{Tr}\,(g_\varphi^2)^*. \end{aligned} \tag{B.4}$$

Since g_φ is Hermitian and hence $g_\varphi^* = g_\varphi^T$, this is simplified to the expression in (3.17), noting $\mathrm{Tr}(A^T) = \mathrm{Tr}\,A$ for any matrix A.

Appendix C. Some useful inequalities

Lemma 1. *For Hermitian matrices* A *and* B,

$$\mathrm{Tr}[(AB)^2] \leqslant \mathrm{Tr}(A^2 B^2). \tag{C.1}$$

The equality holds if and only if $[A,\ B] = 0$.

Proof. Since $\mathrm{i}(AB - BA)$ is Hermitian,

$$\begin{aligned} 0 &\leqslant \mathrm{Tr}\,\{[\mathrm{i}(AB - BA)]^2\} \\ &= -2\,\mathrm{Tr}[(AB)^2] + 2\,\mathrm{Tr}(A^2 B^2). \end{aligned} \tag{C.2}$$

Therefore, the inequality (C.1) follows. The equality holds if and only if $AB - BA = 0$. □

Lemma 2. *For Hermitian matrices* A *and* B,

$$\mathrm{Tr}(A^T B^T AB) \leqslant \mathrm{Tr}(A^2 B^2). \tag{C.3}$$

The equality holds if and only if $AB = (AB)^T$.

Proof. By noting the Hermitianity of A and B,

$$\begin{aligned} 0 &\leqslant \mathrm{Tr}\,\{[AB - (AB)^T]^\dagger [AB - (AB)^T]\} \\ &= 2\,\mathrm{Tr}(A^2 B^2) - 2\,\mathrm{Tr}(A^T B^T AB). \end{aligned} \tag{C.4}$$

Therefore, the inequality (C.3) follows. The equality holds if and only if $AB - (AB)^T = 0$. □

Lemma 3. *For Hermitian and positive semi-definite matrices* A *and* B,

$$\mathrm{Tr}(AB) \leqslant \|A\| \,\mathrm{Tr}\, B, \tag{C.5}$$

where $\|A\|$ *is the spectral norm of* A, *given by its largest eigenvalue. The equality holds if and only if the support of* B *(i.e. the orthogonal complement of its kernel) is contained in the eigenspace of* A *belonging to its largest eigenvalue.*

Proof. Consider the spectral decomposition of the Hermitian and positive semi-definite matrix A,

$$A = \sum_n \lambda_n \boldsymbol{v}_n \boldsymbol{v}_n^\dagger, \qquad \lambda_n \geqslant 0. \tag{C.6}$$

Then, by noting the fact that $\boldsymbol{u}^\dagger B \boldsymbol{u} \geqslant 0$ for any vector $\boldsymbol{u}$,

$$\mathrm{Tr}(AB) = \sum_n \lambda_n \boldsymbol{v}_n^\dagger B \boldsymbol{v}_n \leqslant \lambda_{\max} \sum_n \boldsymbol{v}_n^\dagger B \boldsymbol{v}_n = \lambda_{\max}\, \mathrm{Tr}\, B, \tag{C.7}$$

which proves the statement. The equality holds if and only if $(\lambda_{\max} - \lambda_n)\boldsymbol{v}_n^\dagger B \boldsymbol{v}_n = 0$ for all n, i.e. if and only if $\boldsymbol{v}_k^\dagger B \boldsymbol{v}_k = 0$ for all $\boldsymbol{v}_k$ belonging to the eigenvalues λ_k of A strictly smaller than $\lambda_{\max}$. This, in turns, is equivalent to the condition that the support of B is in the eigenspace of A belonging to its largest eigenvalue $\lambda_{\max}$. □

Lemma 4. *For Hermitian and positive semi-definite matrix* A,

$$\mathrm{Tr}(A^2) \leqslant (\mathrm{Tr}\, A)^2 . \tag{C.8}$$

The equality holds if and only if only one of the eigenvalues of A *is nonvanishing and it is not degenerate.*

Proof. The eigenvalues λ_n of A are positive semi-definite, $\lambda_n \geqslant 0$. Then,

$$\mathrm{Tr}(A^2) = \sum_n \lambda_n^2 \leqslant \left(\sum_n \lambda_n\right)^2 = (\mathrm{Tr}\, A)^2 . \tag{C.9}$$

The equality holds if and only if $\lambda_m \lambda_n = 0$ for all pairs with $m \neq n$, namely, only one of the eigenvalues λ_n is nonvanishing and it is not degenerate. □

Appendix D. Proof of the optimality of the measurement in figure 2

Here, we show that the FI by the optimal input $|\psi_{\mathrm{opt}}\rangle$ in (3.31) and the POVM $\{\hat{\Pi}_x\}$ in (4.7) (the circuit in figure 2) coincides with the upper bound of the QFI in (1.4). To see this, observe that the probability of measuring the value x by this measurement in the output state of the circuit in figure 2 is given by

$$p(x|\varphi) = \langle 0|\, \hat{S}_1^\dagger(r_0) \hat{V}_\varphi^\dagger \hat{U}_\varphi^\dagger \hat{U}_{\varphi'} \hat{V}_{\varphi'} e^{i\theta \hat{a}_1^\dagger \hat{a}_1} |x\rangle_1 \langle x|_1 e^{-i\theta \hat{a}_1^\dagger \hat{a}_1} \hat{V}_\varphi^\dagger \hat{U}_\varphi^\dagger \hat{U}_\varphi \hat{V}_{\varphi'} \hat{S}_1(r_0)|0\rangle, \tag{D.1}$$

where the parameter φ' used in the input state and in the measurement will be set $\varphi' = \varphi$ later. It is the marginal of the Wigner function of the output state along the quadrature $\hat{x}_1 = (\hat{a}_1 + \hat{a}_1^\dagger)/\sqrt{2}$. Its characteristic function $\chi(\xi|\varphi)$ is computed to be

$$\begin{aligned}
\chi(\xi|\varphi) &= \int_{-\infty}^{\infty} \mathrm{d}x\; p(x|\varphi) e^{-i\xi x} \\
&= \langle 0|\, \hat{S}_1^\dagger(r_0) \hat{V}_{\varphi'}^\dagger \hat{U}_\varphi^\dagger \hat{U}_{\varphi'} \hat{V}_{\varphi'} e^{i\theta \hat{a}_1^\dagger \hat{a}_1} e^{-i\xi \hat{x}_1} e^{-i\theta \hat{a}_1^\dagger \hat{a}_1} \hat{V}_{\varphi'}^\dagger \hat{U}_{\varphi'}^\dagger \hat{U}_\varphi \hat{V}_{\varphi'} \hat{S}_1(r_0)|0\rangle \\
&= e^{-\frac{1}{2}(\Delta x)_\theta^2 \xi^2},
\end{aligned} \tag{D.2}$$

where

$$(\Delta x)_\theta^2 = \frac{1}{2}(1 + |(V_{\varphi'}^\dagger U_{\varphi'}^\dagger U_\varphi V_{\varphi'})_{11}|^2 (\cosh 2r_0 - 1) + \mathrm{Re}[e^{-2i\theta}(V_{\varphi'}^\dagger U_{\varphi'}^\dagger U_\varphi V_{\varphi'})_{11}^2] \sinh 2r_0) \tag{D.3}$$

with $(V_{\varphi'}^\dagger U_{\varphi'}^\dagger U_\varphi V_{\varphi'})_{11}$ being the $(1,1)$ element of the matrix $V_{\varphi'}^\dagger U_{\varphi'}^\dagger U_\varphi V_{\varphi'}$. Its Fourier transform yields

$$p(x|\varphi) = \frac{1}{\sqrt{2\pi (\Delta x)_\theta^2}} \exp\left(-\frac{x^2}{2(\Delta x)_\theta^2}\right). \tag{D.4}$$

Then, using (A.22) and (A.23), the associated FI defined by (2.6) becomes

$$\begin{aligned} F(\varphi|\ ,\ |\psi_{\rm opt}\rangle) &= \int_{-\infty}^{\infty} {\rm d}x\ p(x|\varphi)\left(\frac{\partial}{\partial\varphi}\ln p(x|\varphi)\right)^2 \\ &= \frac{1}{2}\left(\frac{\partial}{\partial\varphi}\ln(\Delta x)^2_\theta\right)^2 \\ &= 2\varepsilon_1^2\sinh^2 2r_0\frac{4\sin^2\theta\cos^2\theta}{({\rm e}^{2r_0}\cos^2\theta+{\rm e}^{-2r_0}\sin^2\theta)^2} \end{aligned} \tag{D.5}$$

at $\varphi'=\varphi$, which can be maximized by setting $\theta=\pm\tan^{-1}{\rm e}^{2r_0}$ to get

$$F(\varphi|\mathcal{P},\ |\psi_{\rm opt}\rangle) = 2\varepsilon_1^2\sinh^2 2r_0 = 8\varepsilon_1^2\overline{N}(\overline{N}+1). \tag{D.6}$$

This coincides with the upper bound of the QFI in (1.4), and proves the optimality of the circuit in figure 2.

ORCID iDs

Paolo Facchi https://orcid.org/0000-0001-9152-6515
Kazuya Yuasa https://orcid.org/0000-0001-5314-2780

References

[1] Giovannetti V, Lloyd S and Maccone L 2004 Quantum-enhanced measurements: beating the standard quantum limit *Science* **306** 1330
[2] Giovannetti V, Lloyd S and Maccone L 2006 Quantum metrology *Phys. Rev. Lett.* **96** 010401
[3] Dowling J P 2008 Quantum optical metrology—the lowdown on high-N00N states *Contemp. Phys.* **49** 125
[4] Giovannetti V, Lloyd S and Maccone L 2011 Advances in quantum metrology *Nat. Photon.* **5** 222
[5] Demkowicz-Dobrzański R, Jarzyna M and Kołodyński J 2015 Quantum limits in optical interferometry *Progress in Optics* vol 60 ed E Wolf (Amsterdam: Elsevier) pp 345–435 ch 4
[6] Dowling J P and Seshadreesan K P 2015 Quantum optical technologies for metrology, sensing, and imaging *J. Lightwave Technol.* **33** 2359
[7] Caves C M 1981 Quantum-mechanical noise in an interferometer *Phys. Rev.* D **23** 1693
[8] Bondurant R S and Shapiro J H 1984 Squeezed states in phase-sensing interferometers *Phys. Rev.* D **30** 2548
[9] Yurke B, McCall S L and Klauder J R 1986 SU(2) and SU(1, 1) interferometers *Phys. Rev.* A **33** 4033
[10] Holland M J and Burnett K 1993 Interferometric detection of optical phase shifts at the Heisenberg limit *Phys. Rev. Lett.* **71** 1355
[11] Sanders B C and Milburn G J 1995 Optimal quantum measurements for phase estimation *Phys. Rev. Lett.* **75** 2944
[12] Berry D W and Wiseman H M 2000 Optimal states and almost optimal adaptive measurements for quantum interferometry *Phys. Rev. Lett.* **85** 5098
[13] Pezzé L and Smerzi A 2006 Phase sensitivity of a Mach–Zehnder interferometer *Phys. Rev.* A **73** 011801(R)
[14] Monras A 2006 Optimal phase measurements with pure Gaussian states *Phys. Rev.* A **73** 033821
[15] Uys H and Meystre P 2007 Quantum states for Heisenberg-limited interferometry *Phys. Rev.* A **76** 013804
[16] Pezzé L and Smerzi A 2008 Mach–Zehnder interferometry at the Heisenberg limit with coherent and squeezed-vacuum light *Phys. Rev. Lett.* **100** 073601
[17] Tan S H, Erkmen B I, Giovannetti V, Guha S, Lloyd S, Maccone L, Pirandola S and Shapiro J H 2008 Quantum illumination with Gaussian states *Phys. Rev. Lett.* **101** 253601
[18] Dorner U, Demkowicz-Dobrzański R, Smith B J, Lundeen J S, Wasilewski W, Banaszek K and Walmsley I A 2009 Optimal quantum phase estimation *Phys. Rev. Lett.* **102** 040403
[19] Aspachs M, Calsamiglia J, Muñoz-Tapia R and Bagan E 2009 Phase estimation for thermal Gaussian states *Phys. Rev.* A **79** 033834
[20] Tsang M 2009 Quantum imaging beyond the diffraction limit by optical centroid measurements *Phys. Rev. Lett.* **102** 253601
[21] Anisimov P M, Raterman G M, Chiruvelli A, Plick W N, Huver S D, Lee H and Dowling J P 2010 Quantum metrology with two-mode squeezed vacuum: parity detection beats the Heisenberg limit *Phys. Rev. Lett.* **104** 103602
[22] Hyllus P, Pezzé L and Smerzi A 2010 Entanglement and sensitivity in precision measurements with states of a fluctuating number of particles *Phys. Rev. Lett.* **105** 120501
[23] Escher B M, de Matos Filho R L and Davidovich L 2011 General framework for estimating the ultimate precision limit in noisy quantum-enhanced metrology *Nat. Phys.* **7** 406
[24] Joo J, Munro W J and Spiller T P 2011 Quantum metrology with entangled coherent states *Phys. Rev. Lett.* **107** 083601
[25] Pinel O, Fade J, Braun D, Jian P, Treps N and Fabre C 2012 Ultimate sensitivity of precision measurements with intense Gaussian quantum light: a multimodal approach *Phys. Rev.* A **85** 010101(R)
[26] Jarzyna M and Demkowicz-Dobrzański R 2012 Quantum interferometry with and without an external phase reference *Phys. Rev.* A **85** 011801(R)
[27] Rivas Á and Luis A 2012 Sub-Heisenberg estimation of non-random phase shifts *New J. Phys.* **14** 093052
[28] Genoni M G, Paris M G A, Adesso G, Nha H, Knight P L and Kim M S 2013 Optimal estimation of joint parameters in phase space *Phys. Rev.* A **87** 012107
[29] Monras A 2013 Phase space formalism for quantum estimation of Gaussian states arXiv:1303.3682 [quant-ph]
[30] Pezzé L and Smerzi A 2013 Ultrasensitive two-mode interferometry with single-mode number squeezing *Phys. Rev. Lett.* **110** 163604
[31] Ruo Berchera I, Degiovanni I P, Olivares S and Genovese M 2013 Quantum light in coupled interferometers for quantum gravity tests *Phys. Rev. Lett.* **110** 213601
[32] Zhang X X, Yang Y X and Wang X B 2013 Lossy quantum-optical metrology with squeezed states *Phys. Rev.* A **88** 013838
[33] Lang M D and Caves C M 2013 Optimal quantum-enhanced interferometry using a laser power source *Phys. Rev. Lett.* **111** 173601

[34] Pinel O, Jian P, Treps N, Fabre C and Braun D 2013 Quantum parameter estimation using general single-mode Gaussian states *Phys. Rev.* A **88** 040102(R)
[35] Sahota J and James D F V 2013 Quantum-enhanced phase estimation with an amplified Bell state *Phys. Rev.* A **88** 063820
[36] Jiang Z 2014 Quantum Fisher information for states in exponential form *Phys. Rev.* A **89** 032128
[37] Tan Q S, Liao J Q, Wang X and Nori F 2014 Enhanced interferometry using squeezed thermal states and even or odd states *Phys. Rev.* A **89** 053822
[38] Lang M D and Caves C M 2014 Optimal quantum-enhanced interferometry *Phys. Rev.* A **90** 025802
[39] Knott P A, Proctor T J, Nemoto K, Dunningham J A and Munro W J 2014 Effect of multimode entanglement on lossy optical quantum metrology *Phys. Rev.* A **90** 033846
[40] Sahota J and Quesada N 2015 Quantum correlations in optical metrology: Heisenberg-limited phase estimation without mode entanglement *Phys. Rev.* A **91** 013808
[41] Pezzè L, Hyllus P and Smerzi A 2015 Phase-sensitivity bounds for two-mode interferometers *Phys. Rev.* A **91** 032103
[42] Motes K R, Olson J P, Rabeaux E J, Dowling J P, Olson S J and Rohde P P 2015 Linear optical quantum metrology with single photons: exploiting spontaneously generated entanglement to beat the shot-noise limit *Phys. Rev. Lett.* **114** 170802
[43] Sparaciari C, Olivares S and Paris M G A 2015 Bounds to precision for quantum interferometry with Gaussian states and operations *J. Opt. Soc. Am.* B **32** 1354
[44] Rigovacca L, Farace A, De Pasquale A and Giovannetti V 2015 Gaussian discriminating strength *Phys. Rev.* A **92** 042331
[45] Šafránek D, Lee A R and Fuentes I 2015 Quantum parameter estimation using multi-mode Gaussian states *New J. Phys.* **17** 073016
[46] Friis N, Skotiniotis M, Fuentes I and Dür W 2015 Heisenberg scaling in Gaussian quantum metrology *Phys. Rev.* A **92** 022106
[47] De Pasquale A, Facchi P, Florio G, Giovannetti V, Matsuoka K and Yuasa K 2015 Two-mode bosonic quantum metrology with number fluctuations *Phys. Rev.* A **92** 042115
[48] Gao Y and Wang R M 2016 Variational limits for phase precision in linear quantum optical metrology *Phys. Rev.* A **93** 013809
[49] Sparaciari C, Olivares S and Paris M G A 2016 Gaussian-state interferometry with passive and active elements *Phys. Rev.* A **93** 023810
[50] Knott P A, Proctor T J, Hayes A J, Cooling J P and Dunningham J A 2016 Practical quantum metrology with large precision gains in the low-photon-number regime *Phys. Rev.* A **93** 033859
[51] Gao Y 2016 Quantum optical metrology in the lossy SU(2) and SU(1, 1) interferometers *Phys. Rev.* A **94** 023834
[52] Tsang M, Nair R and Lu X M 2016 Quantum theory of superresolution for two incoherent optical point sources *Phys. Rev.* X **6** 031033
[53] Sahota J, Quesada N and James D F V 2016 Physical resources for optical phase estimation *Phys. Rev.* A **94** 033817
[54] Volkoff T J 2016 Optimal and near-optimal probe states for quantum metrology of number-conserving two-mode bosonic Hamiltonians *Phys. Rev.* A **94** 042327
[55] Gagatsos C N, Branford D and Datta A 2016 Gaussian systems for quantum-enhanced multiple phase estimation *Phys. Rev.* A **94** 042342
[56] Nair R and Tsang M 2016 Far-field superresolution of thermal electromagnetic sources at the quantum limit *Phys. Rev. Lett.* **117** 190801
[57] Lupo C and Pirandola S 2016 Ultimate precision bound of quantum and subwavelength imaging *Phys. Rev. Lett.* **117** 190802
[58] Oszmaniec M, Augusiak R, Gogolin C, Kołodyński J, Acín A and Lewenstein M 2016 Random bosonic states for robust quantum metrology *Phys. Rev.* X **6** 041044
[59] Šafránek D and Fuentes I 2016 Optimal probe states for the estimation of Gaussian unitary channels *Phys. Rev.* A **94** 062313
[60] Jarzyna M and Zwierz M 2017 Parameter estimation in the presence of the most general Gaussian dissipative reservoir *Phys. Rev.* A **95** 012109
[61] Nichols R, Liuzzo-Scorpo P, Knott P A and Adesso G 2018 Multiparameter Gaussian quantum metrology *Phys. Rev.* A **98** 012114
[62] Braun D, Adesso G, Benatti F, Floreanini R, Marzolino U, Mitchell M W and Pirandola S 2018 Quantum-enhanced measurements without entanglement *Rev. Mod. Phys.* **90** 035006
[63] Spedalieri G, Lupo C, Braunstein S L and Pirandola S 2019 Thermal quantum metrology in memoryless and correlated environments *Quantum Sci. Technol.* **4** 015008
[64] Šafránek D 2019 Estimation of Gaussian quantum states *J. Phys. A: Math. Theor.* **52** 035304
[65] Bouwmeester D 2004 Quantum physics: high NOON for photons *Nature* **429** 139
[66] Nagata T, Okamoto R, O'Brien J L, Sasaki K and Takeuchi S 2007 Beating the standard quantum limit with four-entangled photons *Science* **316** 726
[67] Higgins B L, Berry D W, Bartlett S D, Wiseman H M and Pryde G J 2007 Entanglement-free Heisenberg-limited phase estimation *Nature* **450** 393
[68] O'Brien J L, Furusawa A and Vuckovic J 2009 Photonic quantum technologies *Nat. Photon.* **3** 687
[69] Brida G, Genovese M and Ruo Berchera I 2010 Experimental realization of sub-shot-noise quantum imaging *Nat. Photon.* **4** 227
[70] Afek I, Ambar O and Silberberg Y 2010 High-NOON states by mixing quantum and classical light *Science* **328** 879
[71] Kacprowicz M, Demkowicz-Dobrzański R, Wasilewski W, Banaszek K and Walmsley I A 2010 Experimental quantum-enhanced estimation of a lossy phase shift *Nat. Photon.* **4** 357
[72] Xiang G Y, Higgins B L, Berry D W, Wiseman H M and Pryde G J 2011 Entanglement-enhanced measurement of a completely unknown optical phase *Nat. Photon.* **5** 43
[73] Krischek R, Schwemmer C, Wieczorek W, Weinfurter H, Hyllus P, Pezzé L and Smerzi A 2011 Useful multiparticle entanglement and sub-shot-noise sensitivity in experimental phase estimation *Phys. Rev. Lett.* **107** 080504
[74] Genoni M G, Olivares S, Brivio D, Cialdi S, Cipriani D, Santamato A, Vezzoli S and Paris M G A 2012 Optical interferometry in the presence of large phase diffusion *Phys. Rev.* A **85** 043817
[75] Crespi A, Lobino M, Matthews J C F, Politi A, Neal C R, Ramponi R, Osellame R and O'Brien J L 2012 Measuring protein concentration with entangled photons *Appl. Phys. Lett.* **100** 233704
[76] Wolfgramm F, Vitelli C, Beduini F A, Godbout N and Mitchell M W 2013 Entanglement-enhanced probing of a delicate material system *Nat. Photon.* **7** 28
[77] Taylor M A, Janousek J, Daria V, Knittel J, Hage B, Bachor H A and Bowen W P 2013 Biological measurement beyond the quantum limit *Nat. Photon.* **7** 229
[78] Ono T, Okamoto R and Takeuchi S 2013 An entanglement-enhanced microscope *Nat. Commun.* **4** 2426
[79] Vidrighin M D, Donati G, Genoni M G, Jin X M, Kolthammer W S, Kim M S, Datta A, Barbieri M and Walmsley I A 2014 Joint estimation of phase and phase diffusion for quantum metrology *Nat. Commun.* **5** 3532
[80] Israel Y, Rosen S and Silberberg Y 2014 Supersensitive polarization microscopy using NOON states of light *Phys. Rev. Lett.* **112** 103604
[81] Rozema L A, Bateman J D, Mahler D H, Okamoto R, Feizpour A, Hayat A and Steinberg A M 2014 Scalable spatial superresolution using entangled photons *Phys. Rev. Lett.* **112** 223602

[82] Braunstein S L and van Loock P 2005 Quantum information with continuous variables *Rev. Mod. Phys.* **77** 513
[83] Weedbrook C, Pirandola S, García-Patrón R, Cerf N J, Ralph T C, Shapiro J H and Lloyd S 2012 Gaussian quantum information *Rev. Mod. Phys.* **84** 621
[84] Adesso G, Ragy S and Lee A R 2014 Continuous variable quantum information: Gaussian states and beyond *Open Syst. Inf. Dyn.* **21** 1440001
[85] Helstrom C W 1976 *Quantum Detection and Estimation Theory* (New York: Academic)
[86] Braunstein S L and Caves C M 1994 Statistical distance and the geometry of quantum states *Phys. Rev. Lett.* **72** 3439
[87] Braunstein S L, Caves C M and Milburn G J 1996 Generalized uncertainty relations: theory, examples, and Lorentz invariance *Ann. Phys.* **247** 135
[88] Hayashi M 2005 *Asymptotic Theory of Quantum Statistical Inference: Selected Papers* (Singapore: World Scientific)
[89] Paris M G A 2009 Quantum estimation for quantum technology *Int. J. Quant. Inf.* **7** 125
[90] Holevo A S 2011 *Probabilistic and Statistical Aspects of Quantum Theory* (Pisa: Edizioni della Normale)
[91] Nielsen M A and Chuang I L 2000 *Quantum Computation and Quantum Information* (Cambridge: Cambridge University Press)
[92] Hayashi M, Ishizaka S, Kawachi A, Kimura G and Ogawa T 2015 *Introduction to Quantum Information Science* (Berlin: Springer)
[93] Banchi L, Braunstein S L and Pirandola S 2015 Quantum fidelity for arbitrary Gaussian states *Phys. Rev. Lett.* **115** 260501
[94] Fujiwara A 2001 Quantum channel identification problem *Phys. Rev.* A **63** 042304
[95] Yuan H and Fung C H F 2015 Optimal feedback scheme and universal time scaling for Hamiltonian parameter estimation *Phys. Rev. Lett.* **115** 110401
[96] Ballester M A 2004 Entanglement is not very useful for estimating multiple phases *Phys. Rev.* A **70** 032310
[97] Proctor T J, Knott P A and Dunningham J A 2018 Multiparameter estimation in networked quantum sensors *Phys. Rev. Lett.* **120** 080501
[98] Matsuoka K 2015 *Master's Thesis* Waseda University Tokyo (in Japanese)